1988

Diffusion In Strong And Weak Mixed Electrolyte Solutions

Robert Alexander Noulty

NOTICE

The quality of this microform is heavily dependent upon the quality of the original thesis submitted for microfilming. Every effort has been made to ensure the highest quality of reproduction possible.

If pages are missing, contact the university which granted the degree.

Some pages may have indistinct print especially if the original pages were typed with a poor typewriter ribbon or if the university sent us an inferior photocopy.

Previously copyrighted materials (journal articles, published tests, etc.) are not filmed.

Reproduction in full or in part of this microform is governed by the Canadian Copyright Act, R.S.C. 1970, c. C-30.

AVIS

La qualité de cette microforme dépend grandement de la qualité de la thèse soumise au microfilmage. Nous avons tout fait pour assurer une qualité supérieure de reproduction.

S'il manque des pages, veuillez communiquer avec l'université qui a conféré le grade.

La qualité d'impression de certaines pages peut laisser à désirer, surtout si les pages originales ont été dactylographiées à l'aide d'un ruban usé ou si l'université nous a fait parvenir une photocopie de qualité inférieure.

Les documents qui font déjà l'objet d'un droit d'auteur (articles de revue, tests publiés, etc.) ne sont pas microfilmés.

La reproduction, même partielle, de cette microforme est soumise à la Loi canadienne sur le droit d'auteur, SRC 1970, c. C-30.

DIFFUSION IN STRONG AND WEAK MIXED ELECTROLYTE SOLUTIONS

by

Robert Alexander Noulty

Department of Chemistry

Submitted in partial fulfillment of the
requirements for the degree of
Doctor of Philosophy

Faculty of Graduate Studies
The University of Western Ontario
London, Ontario
September 1987

ISBN 0-315-40784-0

ABSTRACT

Binary diffusion coefficients of dilute aqueous lithium, sodium and potassium hydroxides have been determined at 25°C by a simplified version of Harned's conductimetric technique. The large difference in mobility between OH^- and the cations leads to an electrophoretic effect which reduces the rate of diffusion. Measured and predicted diffusion coefficients are in excellent agreement. Diffusion-derived activity coefficients are compared with activity data obtained from emf methods.

A matrix diagonalization procedure has been developed to determine multicomponent diffusion coefficients. If linear combinations of data from multicomponent diffusion experiments with different initial concentration gradients are analyzed as simple binary data, certain combinations can be found that transform the multicomponent diffusion coefficient matrix D to diagonal form and thus yield time-invariant pseudo-binary diffusion coefficients: the eigenvalues of D. Because the matrix that diagonalizes D is given by the coefficients used to form the linear combinations, D can be obtained by the inverse transformation. As a test, ternary diffusion coefficients for aqueous NaOH + NaCl mixtures were determined. The multicomponent diffusivity of the NaOH

component is much larger than its binary diffusivity, and flow of the base produces large coupled flows of NaCl.

Diffusion coefficients of copper sulfate + sulfuric acid + water mixtures have been determined at 25°C using conductimetric and diaphragm cell techniques. Diffusion of sulfuric acid produces large counterflows of copper sulfate and vice versa. If diffusion of copper sulfate in sulfuric acid solutions is treated as a binary process, the measured apparent diffusivities of copper sulfate are 1 to 8% lower than the salt's true diffusivity. Expressions are developed to predict ternary transport coefficients for the mixtures.

The diaphragm cell technique has been used to measure the nine quaternary diffusion coefficients for three compositions of the system KCl + KH_2PO_4 + H_3PO_4 + H_2O at 25°C. It is shown that pH gradients in KH_2PO_4 + H_3PO_4 buffers can drive large coupled flows of KCl which concentrate KCl within diffusion boundaries. Onsager's reciprocal relations for isothermal quaternary diffusion are tested and verified. By transformation of the transport coefficients for the system KCl + KH_2PO_4 + H_3PO_4 + H_2O, coefficients for the system KCl + KH_2PO_4 + HCl + H_2O are obtained.

ACKNOWLEDGEMENTS

My deepest thanks must be given to Dr. D.G. Leaist for his frequent advice and encouragement. I must also thank Dr. P.A. Lyons of Yale University for the loan of the Stokes diffusion cells and conductivity bridge. Thanks to Anne Leaist for typing this thesis and to Anita Elworthy for final preparation of the figures. Lastly, I must thank my wife, Elizabeth, for her patience and understanding, and for her help in the preparation of this thesis.

TABLE OF CONTENTS

LIST OF TABLES

LIST OF FIGURES

LIST OF APPENDICES

CHAPTER ONE

INTRODUCTION

Diffusion is the transfer of matter, in the absence of bulk flow, driven by chemical potential gradients. This movement of material plays an essential role in chemical, geological and biological systems. Interpretation of these mass transport processes requires accurate diffusion data.

Binary diffusion of a single solute in a two component system can be described by one diffusion coefficient, D, corresponding to one independent diffusional flow. In multicomponent systems, diffusional flows of the various components interact. In these systems, diffusion is described by four or more D_{ik}, multicomponent diffusion coefficients, corresponding to two or more independent flows. A ternary system consisting of solvent and two solute components, for example, has two independent flows and is characterized by four D_{ik} coefficients. D_{11} and D_{22} describe the flows of the two components in response to their own concentration gradients. The cross-coefficients D_{12} and D_{21} describe the flow of component 1 per unit concentration gradient in component 2 and the flow of component 2 per unit concentration gradient in component 1, respectively. A

quaternary system (four components) has three independent flows and nine D_{ik} coefficients.

Unlike binary systems in which solute flows are from regions of high concentration to low concentration, coupled diffusion in multicomponent systems can cause components to diffuse up their own concentration gradients. Other interesting effects can occur, such as the increased flow of one component by the addition of another component.

Although a great deal of diffusion data have been reported already, accurate diffusivities of many important electrolytes are still not available, especially for mixed electrolytes. This research was undertaken to measure diffusion coefficients for binary and multicomponent electrolyte solutions. The binary systems which were studied include aqueous alkali metal hydroxides; the multicomponent systems include both ternary (NaOH + NaCl + H_2O and $CuSO_4$ + H_2SO_4 + H_2O) and quaternary (KCl + KH_2PO_4 + H_3PO_4 + H_2O) systems.

Two experimental methods were employed: Stokes diaphragm cell[1,2a] method and a simplified version[3] of Harned's conductimetric technique.[4] In the former method, diffusion is restricted to the pores of a sintered-glass diaphragm that separates the two compartments of the cell. By analyzing the initial and final concentration gradients across the diaphragm, the rate of diffusion is obtained. The conductimetric technique involves creating a small concentration gradient by injecting solution into the

bottom of a column of solution. The flow of electrolyte is then followed by measuring the change in electrical resistance at two pairs of platinum electrodes set into the cell wall.

The diaphragm cell technique, by restricting diffusion to the pores of the diaphragm, eliminates the effects of convectional mixing. However, because of errors due to cell calibration, surface transport effects and conversion of experimentally obtained integral diffusion coefficients to differential values, the accuracy of the diaphragm cell data is limited to about 1%. In contrast, the Harned technique yields the more easily interpolated differential coefficients directly. Convection and temperature variation (conductivity changes about 2% per Kelvin) can have a significant effect upon Harned experiments, especially those of long duration involving dilute solutions. The accuracy of conductimetric diffusion data is limited to 0.3-0.5% for binary systems, slightly higher for ternary systems. The Harned technique can also be easily automated using an automatic balancing resistance bridge, a switch control unit and a small computer. Automation of the diaphragm cell experiment would prove much more difficult.

Because precise conductivity measurements can be made down to very low concentrations, Harned's technique is the method of choice for studies of diffusion of dilute electrolytes. For evaluation of multicomponent

diffusivities, Stokes diaphragm cell technique is the easiest method to use. Since concentration differences of each solute component are determined directly, determination of the D_{ik} coefficients is relatively simple. Unfortunately, as a result of ionic adsorption on the diaphragm, diaphragm cell data are accurate only for solutions with total electrolyte concentration greater than 0.05 mol dm^{-3}. For solutions of lower total concentration, the Harned technique is usually employed.

The remainder of this work will describe the transport equations for electrolyte diffusion and give both experimental data and theoretical predictions for each system studied.

CHAPTER TWO

TRANSPORT EQUATIONS FOR ELECTROLYTE DIFFUSION

2.1 Introduction

In a binary electrolyte solution, the condition of electroneutrality requires the anions to diffuse at the same rate as the cations; diffusion of the ions induces an electric field which slows the more mobile ions and speeds up the less mobile ions. In multicomponent solutions however, the more mobile ions can diffuse more rapidly than the less mobile ions. Electroneutrality is maintained because the electric field can drive coupled flows of other ions in solution.

Suppose an electrolyte solution at constant temperature and pressure contains n solute species which undergo n_r chemical reactions. If the rates of the chemical reactions are rapid compared to the rate of diffusion, which is usually the case, local equilibrium exists. The n_r chemical reactions and the electroneutrality restriction provide $n_r + 1$ constraints on the flows of the species. Therefore, only $N = n - n_r - 1$ diffusional flows[5] are linearly independent. Hence the number of diffusion coefficients required to describe the diffusional properties of the system is N^2.

2.2 Fick's Laws

The movement of component i may be expressed in terms of the flux, J_i, which is defined as the quantity of solute crossing the unit surface area of a plane perpendicular to the direction of flow in unit time. If the solute molecules at concentration, C_i, are moving with average velocity, v_i, perpendicular to the surface considered, the flux can be written as

$$J_i = v_i C_i \qquad (2.2.1)$$

For binary diffusion of a single solute component along the x-coordinate, the flux can also be expressed as[6]

$$J = -D(\partial C/\partial x) \qquad (2.2.2)$$

which is Fick's first law. If J is expressed in moles m^{-2} s^{-1}, x in m, and C in mol m^{-3}, the diffusion coefficient D will be expressed in m^2 s^{-1}. For binary diffusion in three dimensions, equation (2.2.2) takes the form

$$J = -D\nabla C \qquad (2.2.3)$$

where ∇ denotes the gradient operator. Usually the flux J is not measured directly; one measures the change in concentration with time at various points.

Consider a flow of solute occurring in the positive x direction in a diffusion channel of uniform cross-sectional area A. The channel is intersected by two planes of unit area normal to the x-axis situated at x and x + δx respectively. The quantity of matter entering in time δt is J(x)Aδt whereas the quantity leaving through the plane at x + δx in the same time is J(x+δx)Aδt. By using a Taylor expansion, the expression

$$J(x+\delta x)A\delta t = \left(J(x) + \frac{\partial J(x)}{\partial x}\,\delta x\right)A\delta t \qquad (2.2.4)$$

can be written. The net gain of material is then

$$A\delta C\delta x = J(x)A\delta t - \left(J(x) + \frac{\partial J(x)}{\partial x}\,\delta x\right)A\delta t \qquad (2.2.5)$$

or

$$A\delta C\delta x = -\frac{\partial J(x)}{\partial x}\,\delta x A\delta t \qquad (2.2.6)$$

By simplifying the terms and considering the time and distance to approach zero, the equation of continuity is obtained.

$$\frac{\partial C}{\partial t} = -\frac{\partial J(x)}{\partial x} \qquad (2.2.7)$$

Then by substituting equation (2.2.2) into equation (2.2.7) one obtains

$$\frac{\partial C}{\partial t} = \frac{\partial}{\partial x}\left(D\frac{\partial C}{\partial x}\right) \qquad (2.2.8)$$

If the diffusion coefficient is independent of the concentration and therefore of position, then

$$\partial C/\partial t = D(\partial^2 C/\partial x^2) \qquad (2.2.9)$$

which is Fick's second law. For three dimensional binary diffusion, equation (2.2.9) can be rewritten as

$$\partial C/\partial t = D\nabla^2 C \qquad (2.2.10)$$

where ∇^2 denotes the Laplacian operator.

It is sometimes more useful to relate the flux of matter to the gradient in chemical potential instead of the concentration gradient. Hence equation (2.2.2) is rewritten as

$$J = -L(\partial\mu/\partial x) \qquad (2.2.11)$$

or, in three dimensional form,

$$J = -L\nabla\mu \qquad (2.2.12)$$

where L is the Onsager transport coefficient and μ is the chemical potential. Combining equations (2.2.2) and (2.2.11) gives the relationship between D and L.

$$D = L(\partial\mu/\partial C) \qquad (2.2.13)$$

2.3 Binary, Strong Electrolytes

Because diffusion is characterized by zero flow of electric charge, the anions and cations in a binary electrolyte solution must move with the same velocity. Therefore diffusion of a single, strong 1:1 electrolyte is a binary process described by a single diffusion coefficient.

The flux density for the anions and cations can be written as

$$-j_i = \ell_{i1}\nabla\tilde{\mu}_1 + \ell_{i2}\nabla\tilde{\mu}_2 \qquad (2.3.1)$$

where ℓ_{ik} are the Onsager transport coefficients for the ions and $\nabla\tilde{\mu}_k$ the electrochemical potential gradient for ion k.

The Onsager reciprocal relation[7,8] specifies that

$$\ell_{12} = \ell_{21} \qquad (2.3.2)$$

From the electroneutrality restriction, both ions must move with the same velocity

$$j_1 = j_2 \qquad (2.3.3)$$

Stoichiometry gives

$$J = j_1 = j_2 \qquad (2.3.4)$$

The chemical potential of a strong 1:1 electrolyte is given by the sum of the electrochemical potentials, $\tilde{\mu}_i$, of the individual ions. For each ion

$$\tilde{\mu}_i = \tilde{\mu}_i^{\circ} + RT\ln c_i y_i + z_i F\Phi \qquad (2.3.5)$$

where $\tilde{\mu}_i^{\circ} + RT\ln c_i y_i$ and $z_i F\Phi$ are the chemical and electrical contributions to the total potential. z_i, c_i and y_i are the valence, concentration and activity coefficient of ion i. F is the Faraday and Φ is the electric potential. The force that ion i experiences may be written as the gradient of the ion's electrochemical potential

$$-\nabla\tilde{\mu}_i = (-RT/c_i y_i)\nabla(c_i y_i) - z_i F\nabla\Phi \qquad (2.3.6)$$

Substituting equations (2.3.1)-(2.3.6) into equation (2.2.12), yields an expression for the Onsager coefficient L in terms of the ionic ℓ_{ik} coefficients

$$L = (\ell_{11}\ell_{22}-\ell_{21}\ell_{12})/(\ell_{11}+\ell_{22}-\ell_{12}-\ell_{21}) \qquad (2.3.7)$$

In dilute solutions, the cross-coefficients ℓ_{ik} are very small and can usually be neglected.[9] Hence equation (2.3.1) can be rewritten as

$$-j_i = \ell_{ii}\nabla\tilde{\mu}_i \qquad (2.3.8)$$

The mobility u_i of ion i is defined as the velocity per unit driving force[2b]

$$u_i = -v_i/\nabla\tilde{\mu}_i \qquad (2.3.9)$$

But since the flux density j_i of ion i is related to its velocity v_i by equation (2.2.1) the mobility can also be given by

$$u_i = -j_i/(c_i\nabla\tilde{\mu}_i) \qquad (2.3.10)$$

Provided the solution is dilute

$$u_i = D_i/RT \qquad (2.3.11)$$

where D_i is the diffusion coefficient for ion i.

Therefore, from equations (2.3.8) and (2.3.10)-(2.3.11), we have[9]

$$\ell_{ii} = c_i u_i = c_i D_i/RT \qquad (2.3.12)$$

In dilute solutions, equation (2.3.7) becomes

$$L = \frac{C}{RT} D_1D_2/(D_1+D_2) \qquad (2.3.13)$$

For a very dilute solution of a strong 1:1 electrolyte, the electrolyte's chemical potential is given by

$$\mu = \mu^{\circ} + RT\ell nC^2 \qquad (2.3.14)$$

and hence

$$\partial\mu/\partial C = 2RT/C \qquad (2.3.15)$$

Equations (2.2.13), (2.3.13) and (2.3.15) give

$$D^{\circ} = 2D_1D_2/(D_1+D_2) \qquad (2.3.16)$$

which is the limiting Nernst diffusion coefficient, the harmonic average of the diffusion coefficients of the individual ions.

For non-zero electrolyte concentrations, the chemical potential of the solute is given by

$$\mu = \mu^{\circ} + RT\ell n(Cy_{\pm})^2 \qquad (2.3.17)$$

where $y_{\pm}$ is the mean ionic activity coefficient in the molar concentration scale. Differentiation of equation (2.3.17) with respect to C

$$\partial\mu/\partial C = (2RT/C)(1 + C\partial\ell ny_{\pm}/\partial C) \qquad (2.3.18)$$

together with equations (2.2.13), (2.3.13) and (2.3.16) yields

$$D = D^{\circ}(1 + C\partial \ln y_{\pm}/\partial C) \qquad (2.3.19)$$

the expression for the diffusion coefficient of a binary 1:1 strong electrolyte. As the solute concentration approaches zero, equation (2.3.16) is obtained.

When an ion moves in solution, it tends to drag along with it solvent molecules. Hence, the other ions, depending on their relative direction of motion, are moving either with or against the solvent flow. As a result, the other ions are either sped up or slowed down. To take into account these ionic interactions,[2c] small correction terms, Δ_i, are included in equation (2.3.19)

$$D = (D^{\circ}+\Delta_1+\Delta_2)(1 + C\partial \ln y_{\pm}/\partial C) \qquad (2.3.20)$$

where Δ_1 and Δ_2 denote the first and second order electrophoretic corrections. For a 1:1 strong electrolyte, Δ_1 and Δ_2 are given by[2d]

$$\Delta_1 = -\frac{kT}{6\pi\eta}\left(\frac{\lambda_2^{\circ}-\lambda_1^{\circ}}{\lambda_2^{\circ}+\lambda_1^{\circ}}\right)^2 \frac{\kappa}{1+\kappa a} \qquad (2.3.21)$$

and

$$\Delta_2 = -\frac{e^2}{12\pi\eta\epsilon}\left(\frac{\kappa\exp(\kappa a)}{1+\kappa a}\right)^2\left[0.5772 + \ln(2\kappa a) + \sum_{n=1}^{\infty}\frac{(-2\kappa a)^n}{n(n!)}\right] \qquad (2.3.22)$$

where κ, the inverse Debye length in m, is

$$\kappa^2 = \frac{4\pi N e^2}{1000\ \epsilon kT}\sum_i c_i z_i^2 \qquad (2.3.23)$$

a, λ_i, c_i, z_i are the ion size parameter and the limiting conductance, concentration and valence of ion i.
e, k and N are the protonic charge, Boltzmann's constant and Avogadro's constant. T, η, and ϵ are the temperature, viscosity and dielectric constant of the solvent.

In dilute solutions where ionic effects can be ignored, electrophoresis can be neglected. But at higher concentrations, where the electrophoretic effect can amount to several percent of D, these corrections must be included.

2.4 Multicomponent, Strong Electrolytes

To describe diffusion where there is more than one independent solute flux and hence more than one diffusion coefficient, the binary equations introduced in Section 2.3 must be extended. The molar solute fluxes J_i are related to electrolyte concentration gradients ∇C_k by

$$J_i = -\sum_{k=1}^{N} D_{ik}\nabla C_k \qquad (2.4.1)$$

and to solute chemical potential gradients $\nabla\mu_k$ by

$$J_i = -\sum_{k=1}^{N} L_{ik}\nabla\mu_k \qquad (2.4.2)$$

D_{ik} and L_{ik} are related by

$$D_{ik} = \sum_{m=1}^{N} L_{im}\mu_{mk} \qquad (2.4.3)$$

where

$$\mu_{mk} = (\partial\mu_m/\partial C_k)_{T,p,C_{q\neq k}} \qquad (2.4.4)$$

or in matrix form,

$$\underline{D} = \underline{L}\underline{\mu} \qquad (2.4.5)$$

For a mixture of strong electrolytes, $n_r = 0$, and hence $N = n - 0 - 1 = n - 1$ where n is the number of solute species which, in this case, equals s, the number of constituent ions of the electrolytes.

By inverting equation (2.4.2), the expression

$$\nabla(-\mu_i) = \sum_{k=1}^{s-1} R_{ik}J_k \qquad (2.4.6)$$

is obtained. L and R are related by

$$\overline{L} = R^{-1} \qquad (2.4.7)$$

The multicomponent diffusion process can also be described in terms of the flows of the s constituent ions

$$Jm = \sum_{p=1}^{s} \ell_{mp} \nabla(-\tilde{\mu}_p) \qquad (2.4.8)$$

$$\nabla(-\tilde{\mu}_m) = \sum_{p=1}^{s} r_{mp} Jp \qquad (2.4.9)$$

$$l = r^{-1} \qquad (2.4.10)$$

The chemical potential of component i is equal to the sum of the electrochemical potentials of its constituent ions.

$$\mu_i = \sum_{m=1}^{s} \nu_{mi} \tilde{\mu}_m \qquad (2.4.11)$$

Hence

$$\nabla(-\mu_i) = \sum_{m=1}^{s} \nu_{mi} \nabla(-\tilde{\mu}_m) \qquad (2.4.12)$$

The total flow of ion p is equal to the sum of the fluxes of each p-containing component.

$$J_p = \sum_{k=1}^{s-1} \nu_{pk} J_k \qquad (2.4.13)$$

Substitution of equations (2.4.9) and (2.4.13) into equation (2.4.12) leads to

$$\nabla(-\mu_i) = \sum_{k=1}^{s-1} \sum_{m=1}^{s} \sum_{p=1}^{s} \nu_{mi} r_{mp} \nu_{pk} J_k \qquad (2.4.14)$$

Comparing equations (2.4.6) and (2.4.14) shows that

$$R_{ik} = \sum_{m=1}^{s} \sum_{p=1}^{s} \nu_{mi} r_{mp} \nu_{pk} \qquad (2.4.15)$$

or

$$\mathbf{R} = \boldsymbol{\nu}^T \mathbf{r} \boldsymbol{\nu} \qquad (2.4.16)$$

Using equations (2.4.7) and (2.4.10), an expression[5] that relates L_{ik} and ℓ_{ik} can be found.

$$\mathbf{L} = (\boldsymbol{\nu}^T \boldsymbol{\ell}^{-1} \boldsymbol{\nu})^{-1}. \qquad (2.4.17)$$

where ν_{ik} is the stoichiometric coefficient defined as the number of moles of ion i per mole of solute k. ν^T is the transpose of ν.

For example, consider the interdiffusion of two strong electrolytes MX(1) and MY(2) with common ion M. There are s = 3 constituent ions and hence N = 3 - 0 - 1 = 2 independent flows. If the ions are numbered as 1 = X, 2 = M and 3 = Y, then ν will have the form

$$\nu = \begin{pmatrix} 1 & 0 \\ 1 & 1 \\ 0 & 1 \end{pmatrix} \qquad (2.4.18)$$

2.5 Multicomponent, Chemically-reacting Electrolytes

If the diffusing species are chemically reactive, there will be other ions in solution in addition to the s constituent ions. To evaluate the effect of these additional ions on the diffusional properties of the system, we will first write an expression for the molar flux of species p.

$$j_p = -\sum_{q=1}^{n} \ell_{pq} \nabla\mu_q \qquad (2.5.1)$$

where ℓ_{pq} are the transport coefficients of the species and $\nabla\mu_q$ is the electrochemical potential gradient of

species q. A relationship must now be found between l_{pq} and the mobilities of the n species.

Let stoichiometric coefficient ν_{ip} define the number of moles of constituent ion i per mole of species p. The total flow of ion i is equal to the sum of the fluxes of each i-containing species.

$$j_i = \sum_{p=1}^{n} \nu_{ip} j_p \qquad (2.5.2)$$

Substitution of equation (2.5.1) into equation (2.5.2) gives

$$j_i = -\sum_{p=1}^{n} \sum_{q=1}^{n} \nu_{ip}\, l_{pq}\, \nabla\mu_q \qquad (2.5.3)$$

The electrochemical potential gradient per mole of ion q is

$$\nabla\mu_q = \sum_{k=1}^{s} \nu_{kq}\, \nabla\tilde{\mu}_k \qquad (2.5.4)$$

where ν_{kq} is the number of moles of constituent ion k per mole of species q.

Using equation (2.5.4) one may write

$$j_i = -\sum_{k=1}^{s} \sum_{p=1}^{n} \sum_{q=1}^{n} \nu_{ip}\, l_{pq}\, \nu_{kq}\, \nabla\tilde{\mu}_k \qquad (2.5.5)$$

Comparing this result with equation (2.4.8) (setting m = i and p = k), the Onsager coefficients for the ions can be expressed as

$$\ell_{ik} = \sum_{p=1}^{n} \sum_{q=1}^{n} \nu_{ip} \ell_{pq} \nu_{kq} \qquad (2.5.6)$$

or

$$\ell = \nu \, \ell \, \nu^T \qquad (2.5.7)$$

By the use of equation (2.4.17), the Onsager coefficients for the solutes are then given by

$$L = (\nu^T (\nu \, \ell \, \nu^T)^{-1} \nu)^{-1} \qquad (2.5.8)$$

For ideally dilute solutions, the limiting transport coefficients of the species are given by

$$\ell^{\circ}_{ik} = \delta_{ik} c_i \mu^{\circ}_i = \delta_{ik} c_i D^{\circ}_i / RT \qquad (2.5.9)$$

where δ_{ik} is Kronecker's delta. Substitution of equation (2.5.9) into equation (2.5.6) gives

$$\ell^{\circ}_{ik} = \sum_{q=1}^{n} \nu_{iq} \nu_{kq} c_q D^{\circ}_q / RT \qquad (2.5.10)$$

Expressions for the other limiting coefficients are given by

$$L^\circ = (\nu^T \ell^{\circ -1} \nu)^{-1} \qquad (2.5.11)$$

and

$$D^\circ = L^\circ \mu^\circ \qquad (2.5.12)$$

At non-zero concentrations, no exact relationship exists between the ℓ_{ik} coefficients and the ion mobilities.[5] However, the off-diagonal elements of ℓ are much smaller than the diagonal elements.[10] Also the mobilities of the ions vary little with concentration.[2d] This allows us to write the approximation[5]

$$\ell_{ik} = \delta_{ik} c_i D_i / RT \qquad (2.5.13)$$

where D_i is the diffusivity of ion i. D_i values may be calculated from conductivity and transference number experiments, from diffusion data or by theoretical means.[5,11]

The usual procedure to calculate theoretical estimates for the diffusion coefficients is to first evaluate the ℓ_{ik} values from equation (2.5.13) and then the L coefficients from equation (2.5.8). The concentration derivatives of the chemical potentials for each solute are

found and finally the diffusion coefficients are calculated from equation (2.4.3).

It is customary to ignore the electrophoretic and relaxation corrections for a multicomponent system. Because these corrections are usually much smaller than the thermodynamic correction for nonideality, including them is only worthwile when very accurate activity coefficient data are available.[11]

CHAPTER THREE

DIFFUSION OF BINARY, STRONG ELECTROLYTES: DILUTE AQUEOUS SOLUTIONS OF LITHIUM, SODIUM, AND POTASSIUM HYDROXIDES

3.1 Introduction

In this work, diffusion coefficients were measured for dilute aqueous solutions of lithium, sodium and potassium hydroxides using a conductimetric technique. Accurate thermodynamic and diffusional properties of the hydroxides, especially at low concentrations, are needed to correctly interpret several important processes such as the interdiffusion of a base and its salt or an acid and a base.

Emf measurements can be used to determine activity coefficients for aqueous hydroxide solutions. In practice, however, the application of emf methods to hydroxide solutions poses special difficulties.[12-14] Both absorption of carbon dioxide from the atmosphere and leakage of the bridge electrolyte from the silver-silver halide reference electrode into the cell compartment can change the observed emf values. It will be shown that a precise set of activity coefficients for binary hydroxide solutions can be determined from diffusion measurements.

Prior to this work, Fary[15] used Rayleigh interferometry to measure diffusion of aqueous NaOH over the concentration range 0.031-2.18 mol dm^{-3}.

Bhatia et al.[16] have reported data for aqueous KOH determined by a modified Stokes cell constructed from Perspex with a teflon diaphragm from 0.1 mol dm^{-3} up to saturation. No measurements appear to have been reported for the LiOH + H_2O system.

3.2 Harned Conductimetric Technique

In the Harned conductimetric technique,[4] a concentration gradient is formed in a short column of solution. As the diffusion experiment proceeds, changes in concentration are followed by monitoring the changes in electrical resistance with pairs of small platinum electrodes set in the cell wall (see Figure 3.2.1).

Because the difference in solute concentration from the top to the bottom of the cell is small, D may be assumed to be constant allowing us to write

$$\partial C/\partial t = D(\partial^2 C/\partial x^2) \qquad (3.2.1)$$

Because there is no flow of material out of the ends of the cell, the boundary conditions are

$$\partial C/\partial x = 0;\ x = a,\ 0 \qquad (3.2.2)$$

where a is the height of the diffusion column. The solution of equation (3.2.1), which satisfies the boundary conditions, may be written as a Fourier series.

FIGURE 3.2.1: Harned Conductimetric Cell

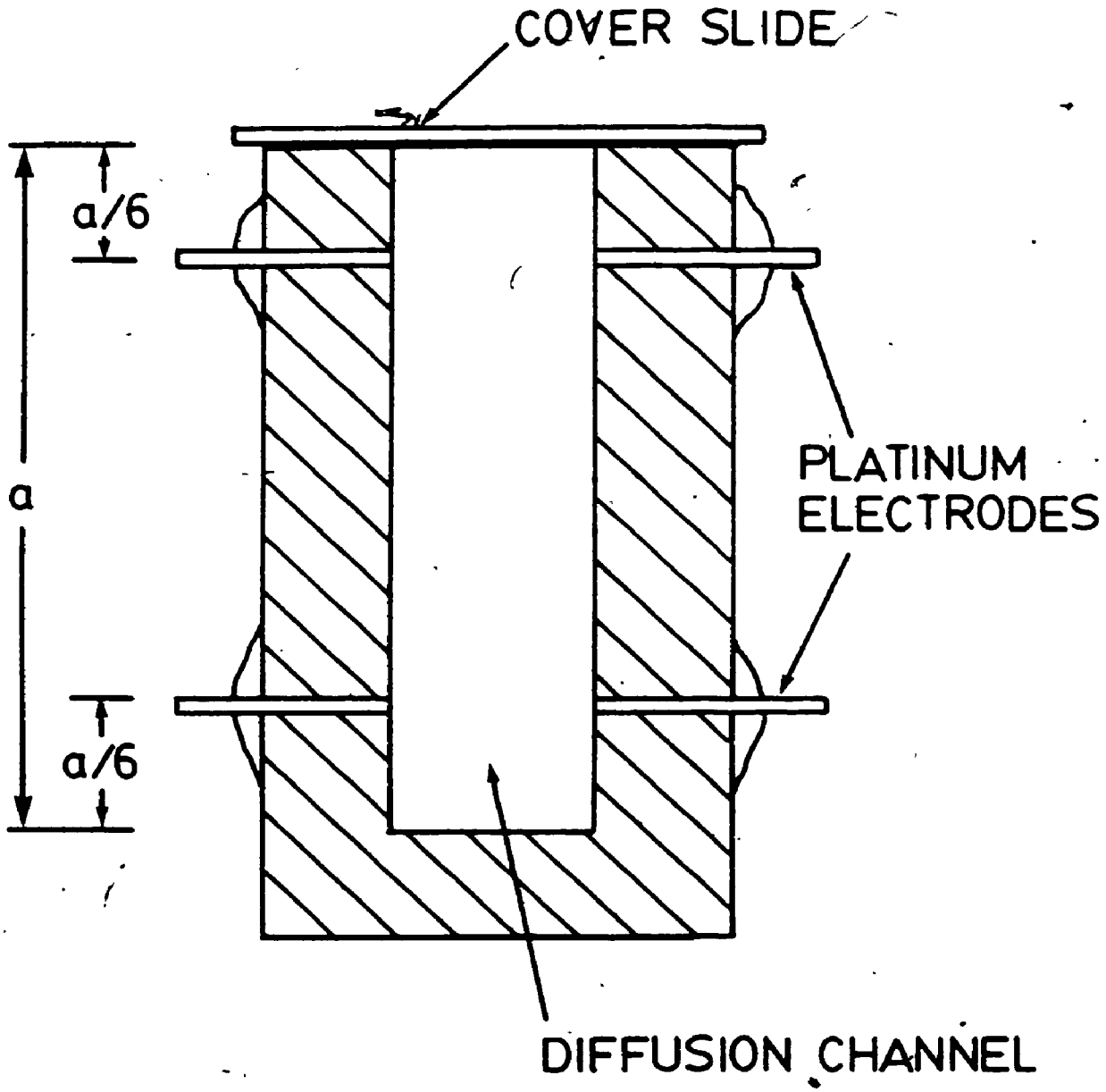
COVER SLIDE
a/6
a
a/6
PLATINUM
ELECTRODES
DIFFUSION CHANNEL

$$C = C_o + \sum_{n=1}^{\infty} A_n \exp(-n^2\pi^2 Dt/a^2) \cos(n\pi x/a) \qquad (3.2.3)$$

where A_n and C_o are constants.

By placing the electrodes at heights a/6 and 5a/6, the difference in concentration of electrolyte is given by

$$C_B(t) - C_T(t) = A_1' \exp(-\pi^2 Dt/a^2) + A_5' \exp(-25\pi^2 Dt/a^2) + \ldots \qquad (3.2.4)$$

where $A_1' = \sqrt{3}\, A_1$, $A_5' = -\sqrt{3}\, A_5$, etc. C_T and C_B are the solute concentrations at the top and bottom reference levels respectively.

Because of the rapid convergence of this series, only the first term is significant after a short time, leaving[2a]

$$\Delta C(t) = A_1' \exp(-\pi^2 Dt/a^2) \qquad (3.2.5)$$

where $\Delta C = C_B - C_T$. By logarithmic differentiation one obtains

$$d\ln[\Delta C(t)]/dt = -\pi^2 D/a^2 \qquad (3.2.6)$$

Thus a plot of $\ln[\Delta C(t)]$ vs t will yield a straight line with slope $-\pi^2 D/a^2$.[2a]

The change in concentration is followed by measuring the change in resistance between the two pairs of electrodes. The resistance R, is related to cell concentration C, cell constant k and molar conductivity Λ by

$$C = k/\Lambda R \qquad (3.2.7)$$

Then

$$\Delta C(t) = (k_B/\Lambda_B R_B) - (k_T/\Lambda_T R_T) \qquad (3.2.8)$$

or

$$\Delta C(t) = (k_B/\bar{\Lambda})((1/R_B) - (r/R_T)) \qquad (3.2.9)$$

where $r = k_T/k_B$ is the ratio of electrode cell constants and $\bar{\Lambda}$ is the molar conductance at the mean cell concentration. Hence, for a strong electrolyte, $\Delta C(t)$ is directly proportional to $\Delta K(t)$, the change in conductivity between the two reference levels at time t.

Equation (3.2.6) can then be rewritten in terms of the conductivity, K, giving

$$D = (-a^2/\pi^2)\, d\ln[\Delta K(t)]/dt \qquad (3.2.10)$$

3.3 Experimental Procedure

The diffusion cells were constructed from high density polyethylene[17] with cylindrical diffusion channels: 0.04572 m height, 0.0126 m diameter. The average cell volume was 5.78×10^{-3} dm^{-3}. Adsorption of ions was minimized by using small platinum electrodes (10^{-3} m diameter) with a light platinum black coating. The cells were initially filled with conductivity water or a dilute hydroxide solution, sealed with a glass slide lubricated with a mixture of Apiezon M grease and vaseline, and placed in a water bath held at 25.00 ± 0.02°C. Initial concentration gradients were then formed by injecting a stock hydroxide solution with a calibrated syringe into the bottom of each cell.

Resistance readings were taken six times a day for four or five days starting one day after the injection procedure. A Leeds and Northrup AC Resistance Bridge was used. Source of the AC signal was a General Radio 1311-A Audio Oscillator set at 2000 Hz. The bridge's sensitivity was controlled by a Geheral Radio 1232-A Tuned Amplifier and Null Detector. Signals from the bridge were displayed on a Telequipment D1011 Oscilloscope.

Stock solutions (1 mol dm^{-3}) were prepared[18] by dilution of filtered saturated solutions of reagent grade hydroxides. The concentrations of the stock hydroxide solutions were determined by potentiometric titration against potassium hydrogen phthalate. Winkler

analyses[15,19,20a] before and after the experiments showed that the solutions contained 0.02-0.05% carbonate based on total alkali. Diffusion experiments performed with carbonate-spiked KOH indicated that the errors caused by carbonate contamination of the stock solutions could be neglected (< 0.1% of D). Solutions were prepared with degassed, twice-distilled, deionized water (conductivity 0.6×10^{-4} ohm^{-1} m^{-1}). Corrections for solvent conductance were negligible.

3.4 Results and Discussion

3.4.1 Diffusion Coefficients

The results of the binary diffusion measurements are summarized in Tables 3.4.1, 3.4.2 and 3.4.3. Attempts to measure diffusion coefficients below 0.002 mol dm^{-3} were unsuccessful because the density gradients were too small to stabilize the diffusion column against convection. Uncertainties in the cell height and cell constant limited the accuracy of the data to 0.3-0.5%.

Diffusion coefficients of binary hydroxide solutions may be predicted by the Onsager-Fuoss expression[2d]

$$D = (D^{\circ}+\Delta_1+\Delta_2)(1 + C\partial \ln y_{\pm}/\partial C) \qquad (3.4.1)$$

for a dilute electrolyte solution. Expressions for D° and Δ_1 and Δ_2 are given by equations (2.3.16) and (2.3.21)-(2.3.23). The ionic diffusivities are calculated from

TABLE 3.4.1

Diffusion Coefficients for Aqueous LiOH Solutions at 25°C

c^b	$D_{obs}{}^b$	$D_{calc}{}^b$
0.00	-	1.721[a]
2.22	1.653	1.664
2.96	1.661	1.657
5.19	1.635	1.639
10.4	1.612	1.612
20.0	1.582	1.581
29.7	1.565	1.558
40.0	1.539	1.540
49.6	1.524	1.526
60.0	1.521	1.512
81.7	1.493	1.489
96.3	1.471	1.476
148.0	1.438	1.439

[a] Equation (2.3.16)

[b] Units: C in 10^{-3} mol dm^{-3}; D in 10^{-9} m^2 s^{-1}

TABLE 3.4.2

Diffusion Coefficients for Aqueous NaOH Solutions at 25°C

C^b	$D_{obs}{}^b$	$D_{calc}{}^b$
0.00	-	2.130[a]
1.66	2.070	2.076
2.48	2.069	2.065
3.31	2.052	2.057
6.62	2.043	2.033
8.28	2.017	2.024
9.95	2.030	2.016
13.3	2.011	2.004
16.6	1.995	1.994
24.8	1.981	1.974
31.2	1.990[c]	1.963
33.1	1.966	1.960
41.4	1.945	1.949
44.8	1.957	1.945
49.7	1.937	1.940
51.5	1.975[c]	1.938
58.1	1.938	1.933
66.2	1.922	1.927
74.5	1.917	1.922
79.5	1.915	1.920
102.6	1.913[c]	1.915

[a] Equation (2.3.16)
[b] Units: C in 10^{-3} mol dm^{-3}; D in 10^{-9} m^2 s^{-1}
[c] Ref. 15

TABLE 3.4.3

Diffusion Coefficients for Aqueous KOH Solutions at 25°C

c^b	$D_{obs}{}^b$	$D_{calc}{}^b$
0.00	-	2.856[a]
1.55	2.781	2.793
3.10	2.765	2.772
4.65	2.752	2.757
9.29	2.739	2.728
20.1	2.720	2.693
29.5	2.689	2.676
43.0	2.677	2.662
49.6	2.660	2.657
62.0	2.655	2.652
74.5	2.663	2.650
77.4	2.640	2.650
101.0	2.646	2.650
103.0	2.680[c]	2.650
119.0	2.640	2.654

[a] Equation (2.3.16)

[b] Units: C in 10^{-3} mol dm^{-3}; D in 10^{-9} m^2 s^{-1}

[c] Ref. 16

$$D_1 = RT\lambda_1^\circ/(z_1F)^2 \qquad (3.4.2)$$

and published limiting molar conductances.[2e] Values of the parameters needed to evaluate D°, Δ_1 and Δ_2 for each of the hydroxides are listed in Table 3.4.4.

Corrections for departures from ideal solution thermodynamics are obtained using activity coefficients calculated by the use of an extended Debye-Huckel expression.[21-23]

$$\ln y_\pm = -\frac{\alpha C^{1/2}}{1+\kappa a} + BC - \ln\left[\frac{\rho(C) + 0.001C(2M_1-M_2)}{\rho(0)}\right] \qquad (3.4.3)$$

where α = 1.176 for aqueous solutions at 25°C. M_1 and M_2 are molar masses of the solvent and solute respectively. $\rho(0)$ and $\rho(C)$ are the densities of the solvent and solution. $\rho(C)$ is calculated from[24a]

$$\rho(C) = \rho(0) + \frac{(M_2-\Phi_V^\circ\rho(0))C}{1000} - \frac{S_V\rho(0)C^{3/2}}{1000} \qquad (3.4.4)$$

where Φ_V° is the standard apparent molar volume at infinite dilution and S_V is the experimental slope for the apparent molar volume.

The term BC in equation (3.4.3) is a correction for short range solute-solvent interactions. By fitting equations (3.4.1) and (3.4.3) to the observed diffusion coefficients (with B as the single adjustable parameter) and averaging,[17] the B values listed in Table 3.4.4 are

TABLE 3.4.4

Supplemental Data[a] for Calculation of Diffusion Coefficients for Dilute Aqueous Hydroxide Solutions at 25°C

Parameter	LiOH	NaOH	KOH
λ_+° [b]/10^4 $m^2 \cdot S\ mol^{-1}$	38.60	50.10	73.50
$10^{10}a$ [c]/m	3.00	3.24	3.70
B/$dm^3\ mol^{-1}$	-0.020	0.036	0.064
Φ_V° [d]/10^6 $m^3\ mol^{-1}$	-6.0	-6.7	2.9
S_V [d]/10^6 $m^3\ mol^{-1}(dm^3\ mol^{-1})^{1/2}$	3.00	4.18	4.35

[a] Limiting conductance[2e] of OH^-, λ_-° = 0.01983 $m^2\ S\ mol^{-1}$; viscosity[2h] of water η = 8.90 x 10^{-4} kg $m^{-1}\ s^{-1}$, density[2h] $\rho(0)$ = 9.9707 x 10^2 kg m^{-3}, dielectric constant[2h] ϵ = 78.3

[b] Ref. 2e

[c] Ref. 24b

[d] Ref. 24a

obtained. Upon substitution of these average B values back into equations (3.4.1) and (3.4.3), the predicted diffusion coefficients shown in Figure 3.4.1 (solid lines) are obtained. Also displayed in Figure 3.4.1 are the experimental diffusion coefficients. Agreement between the calculated and measured diffusion coefficients is excellent, within experimental error over the concentration range studied.

Above 0.03 mol dm^{-3}, the present results for NaOH overlap the optical data of Fary[15] as shown in Figure 3.4.1. The diffusivities at the two lowest concentrations reported by Fary (0.0312 and 0.0515 mol dm^{-3}) are about 2% higher than the conductimetric values. But at low concentrations, optical data can be in error due to the neglect of the concentration dependence of D and the refractive index.[25,26] The conductimetric data also overlap the diaphragm cell data of Bhatia et al.[16] at 0.1 mol dm^{-3}: Usually diaphragm cell experiments yield integral diffusion coefficients: averages of differential coefficients taken over the range of concentration between the upper and lower compartments. Bhatia et al. have converted their data to differential diffusion coefficients using

$$\bar{D} = \frac{1}{t}\int_0^t dt \left[\frac{1}{C'-C''}\right]\int_{C''}^{C'} D\,dC \qquad (3.4.5)$$

FIGURE 3.4.1: Binary Diffusion Coefficients of Dilute Aqueous Hydroxide Solutions at 25°C: solid line, equation (3.4.1); broken line, equation (3.4.1) with electrophoretic corrections omitted; O, this work; +, diaphragm data of Bhatia et al., Ref. 16; Δ, optical data of Fary, Ref. 15; □, limiting Nernst values from equation (2.3.16).

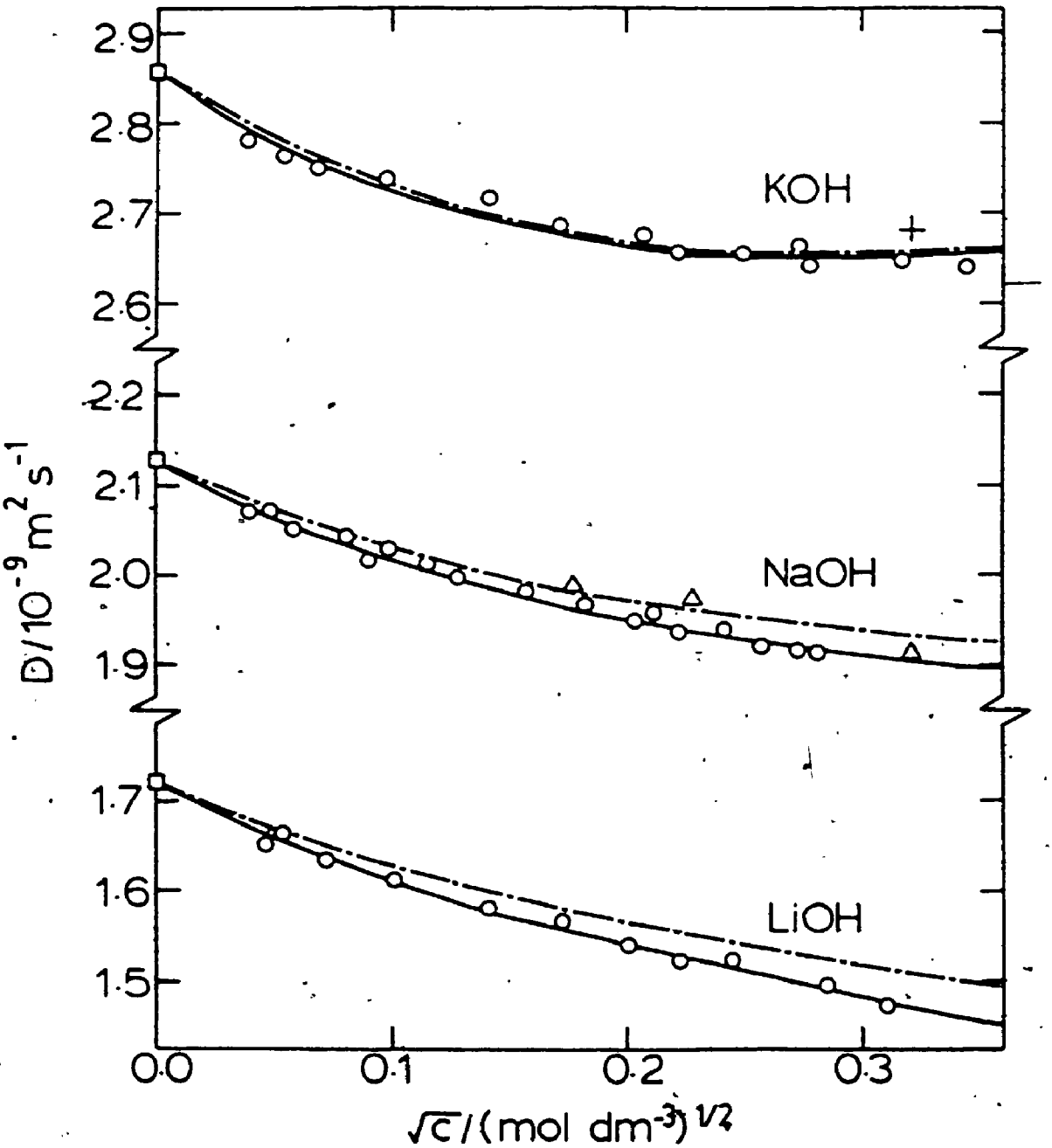
2·9
2·8
2·7
2·6
2·2
2·1
2·0
1·9
1·7
1·6
1·5
KOH
NaOH
LiOH
0·0
0·1
0·2
0·3
D/10⁻⁹ m² s⁻¹
√c/(mol dm⁻³)^1/2

and the method of Stokes.[1] C' and $\bar{C}''$ are the concentrations in the two cell compartments at time t. This conversion allows our results to be compared directly with Bhatia et al's. data. Agreement between the two sets of data is well within experimental error.

Since the conductimetric data agrees with the optical data at higher concentrations and since a short extrapolation of the data gives limiting diffusion coefficients consistent with values predicted by equation (2.3.16), the conductimetric data was considered to be precise and accurate.

Also shown in Figure 3.4.1 (broken lines) are predicted diffusion coefficients calculated by omitting the electrophoretic corrections from equation (3.4.1). Because the differences in the ion mobilities for the hydroxides are unusually large, the first order term Δ_1 is large and negative and overwhelms the smaller positive second term Δ_2. As a result, the net electrophoretic effect is negative. In the series KOH, NaOH, LiOH, the steady increase in $\lambda^{\circ}_{OH^-} - \lambda^{\circ}_{M^+}$ results in a corresponding increase in the magnitude of the electrophoretic effect. For LiOH, for which the effect is largest, the electrophoretic terms can be as much as 3% of D at the higher concentrations.

3.4.2 Activity Coefficients

Experimental activity coefficients for the dilute binary hydroxides shown in Figure 3.4.2 were calculated

FIGURE 3.4.2: Mean Molal Activity Coefficients of Dilute Aqueous Hydroxide Solutions at 25°C. The curves for NaOH and LiOH are displaced downward by 0.1 and 0.2 units, respectively. Curves: ——, this work, equations (3.4.3) and (3.4.4); – – –, Pitzer, equations (3.4.8)-(3.4.11); —·——·——, Guggenheim, equation (3.4.7). KOH data: □, Knobel, Ref. 37; ○, Harned and Cook, Ref. 42; Δ, Scatchard, Ref. 38. NaOH data: □, Harned, Ref. 40; ○, Harned and Hecker, Ref. 41; ▲, Perse, Ref.39; +, from conductance, Corti et al., Ref. 14. LiOH data: □, Harned and Swindells, Ref. 36; +, from conductance, Corti et al., Ref. 14.

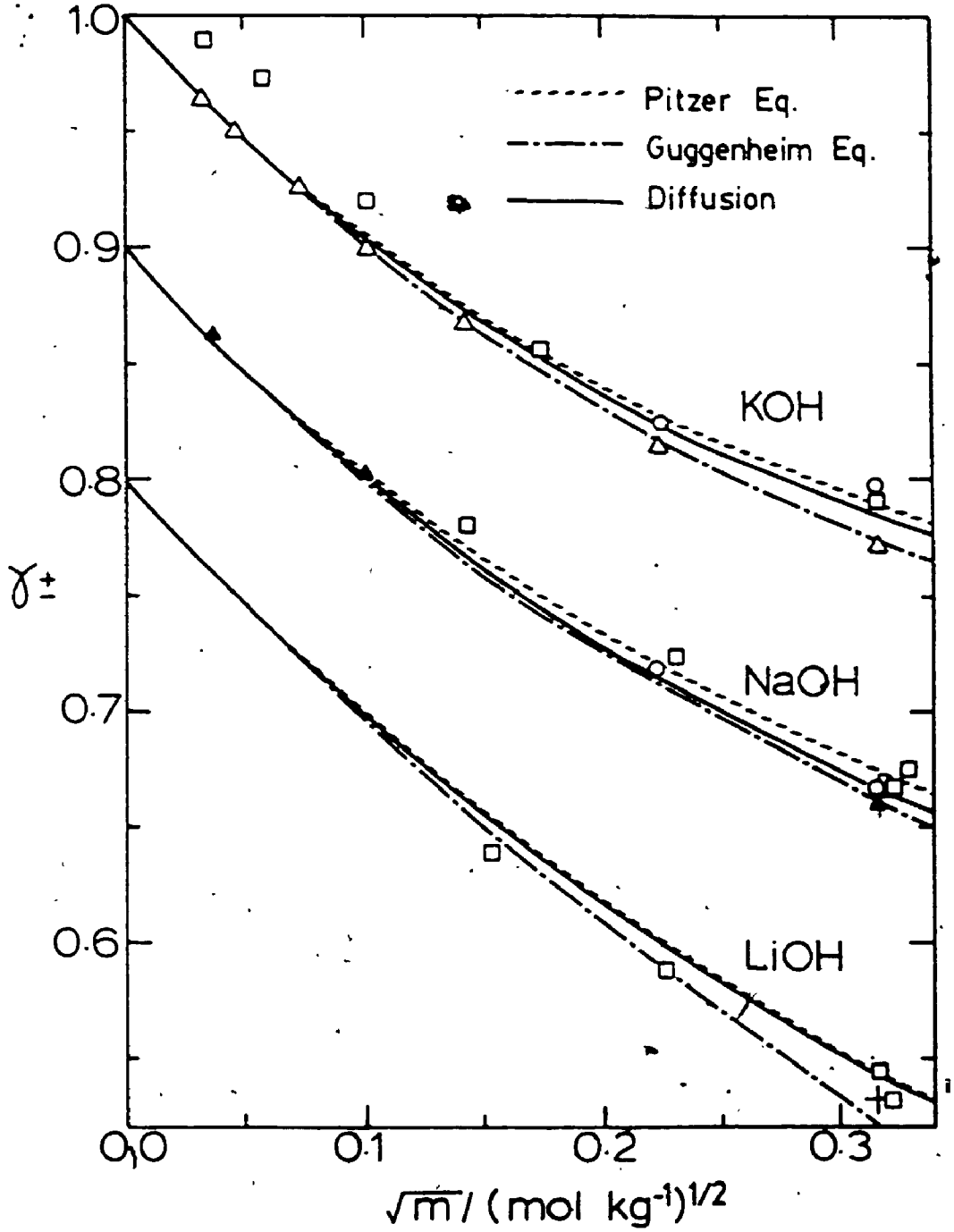
1.0
0.9
0.8
0.7
0.6
γ±
0.0
0.1
0.2
0.3
√m / (mol kg⁻¹)^1/2
Pitzer Eq.
Guggenheim Eq.
Diffusion
KOH
NaOH
LiOH

from equations (3.4.3) and (3.4.4) and the measured B values. The experimentally derived molar-scale activity coefficients $y_\pm$ were converted to the molal-scale activity coefficients $\gamma_\pm$ by utilizing the relationship

$$\gamma_\pm = \frac{C}{m\rho(0)}\, y_\pm \qquad (3.4.6)$$

where m is the molal-scale concentration.

The diffusion derived activity coefficients were compared to activity data calculated by several semiempirical representations (Figure 3.4.2).

The treatment developed by Guggenheim[27] provides an accurate representation of electrolyte activity coefficients. For a 1:1 electrolyte, we have

$$\ln \gamma_{\pm MX} = \frac{-\alpha m^{1/2}}{1 + m^{1/2}} + 2\,\beta_{MX}\, m \qquad (3.4.7)$$

where β_{MX} is a term that represents the net effect of short range forces between the M^+ and X^- ions. From an analysis of emf measurements by Harned et al.[28-31] for mixed electrolyte cells of the type

$$Pt|H_2|MOH,MX|AgCl|Ag$$

where M = Li, Na, or K and X = Cl or Br, Guggenheim and

Turgeon[27] obtained $\beta_{KOH} = 0.13 \pm .0.03$ and $\beta_{NaOH} = 0.06 \pm 0.03$ kg mol^{-1}. For LiOH, the value $\beta_{LiOH} = -0.21 \pm 0.03$ kg mol^{-1} derived by Corti et al.[14] was used.

A more recent treatment of the thermodynamic properties of electrolytes has been developed by Pitzer.[12,32] In the case of a univalent electrolyte, Pitzer's equations reduce to

$$\ln\gamma_{\pm} = f^{\gamma} + mB^{\gamma}_{MX} + m^2C^{\gamma}_{MX} \qquad (3.4.8)$$

$$f^{\gamma} = -A_{\Phi}\left[\frac{m^{1/2}}{1 + bm^{1/2}} + \frac{2}{b}\ln(1 + bm^{1/2})\right] \qquad (3.4.9)$$

$$B^{\gamma}_{MX} = 2B^{(0)}_{MX} + \frac{2B^{(1)}_{MX}}{\alpha^2 m}\left[1-e^{-\alpha m^{1/2}}(1+\alpha m^{1/2}-\tfrac{1}{2}\alpha^2 m)\right] \qquad (3.4.10)$$

$$C^{\gamma}_{MX} = (3/2)C^{\Phi}_{MX} \qquad (3.4.11)$$

Values of the parameters needed to evaluate equations (3.4.8)-(3.4.11) are listed in Table 3.4.5. For KOH and NaOH, the parameters were taken from Pitzer and Mayorga's[12] compilation. The parameters for the aqueous KOH solutions were derived from Akerlof and Bender's[33] emf measurements on cells with amalgam and hydrogen electrodes. The NaOH parameters were based on the isopiestic data of Stokes[34] and the amalgam cell measurements of Akerlof and

TABLE 3.4.5

Supplemental Data[a,c] for Calculation of Activity Coefficients from Pitzer's Equations for Dilute Aqueous Hydroxide Solutions at 25°C

Parameter	LiOH	NaOH	KOH
$B_{MX}^{(0)}$ [b]	0.015	0.0864	0.1298
$B_{MX}^{(1)}$ [b]	0.14	0.253	0.320
C_{MX}^{Φ} [b]	-	0.0044	0.0041

[a] $A_\Phi = 0.392$ (kg mol^{-1})$^{1/2}$, b = 1.2 (kg mol^{-1})$^{1/2}$, $\alpha = 2.0$ (kg mol^{-1})$^{1/2}$

[b] Units: $B_{MX}^{(0)}$ and $B_{MX}^{(1)}$ in kg mol^{-1}; C_{MX}^{Φ} in (kg mol^{-1})^2

[c] Ref. 12, 13

Kegeles.[35] For LiOH, we used the parameter values recommended by Covington, Ferra and Robinson[13] after reanalysis of the amalgam cell data of Harned and Swindells.[36]

As shown in Figure 3.4.2, the diffusion derived activity coefficients agree quite well with the emf data of Knobel,[37] Scatchard,[38] Perse[39] and Harned et al.[36,40-42] and the conductimetric data of Corti et al.[14] Agreement between the diffusion derived activity coefficients and Pitzer's predictions is especially good: within 0.01 unit at 0.1 mol kg^{-1} for each of the three hydroxides studied. Guggenheim's treatment works well for the Na and K hydroxides but the predicted values for LiOH fall slightly below the diffusion results and the $\gamma_\pm$ values calculated from Pitzer's equations.

In deriving the experimental activity coefficients, it was assumed that all three electrolytes were fully ionized. For NaOH and KOH, the strong electrolyte assumption is certainly valid, but conductance studies indicate that LiOH is a weakly associated electrolyte (K_a = 0.9 dm^3 mol^{-1} at 25°C). The error[43] arising from the neglect of ion association can be expressed as

$$\delta y_\pm = 2\,CK_a(D_m-D_i)/D_i \qquad (3.4.12)$$

where C, K_a, D_m and D_i are the concentration, association constant and diffusion coefficient of the associated and

ionized form of the electrolyte. Comparing the diffusion derived activity coefficients with the emf derived data suggests that $\delta y_{\pm}$ is of the order of 0.02 at 0.1 mol dm^{-3} and considerably smaller at lower concentrations. Using this value and equation (3.4.12), the diffusion coefficient of associated LiOH can be calculated to be within 10% of the value for the fully ionized electrolyte. Loss of the unusually large mobility of OH^- on association with Li^+ is partly compensated by an increase in the mobility of the associated LiOH since the ion pair is certainly less hydrated than free Li^+.

3.5 Summary and Conclusions

Binary diffusion coefficients of aqueous lithium, sodium and potassium hydroxides were measured at 25°C from 0.002 to 0.14 mol dm^{-3}. The measured diffusion coefficients were in good agreement with predictions from Onsager-Fuoss transport theory. Precise activity coefficients were determined from diffusion data and compared to activity data evaluated from emf measurements and theoretical treatments. Agreement for the LiOH, NaOH and KOH data was excellent.

CHAPTER FOUR

DIFFUSION OF A BASE AND ITS SALT: AN EIGENVALUE METHOD FOR DETERMINING MULTICOMPONENT DIFFUSION COEFFICIENTS

4.1 Introduction

Multicomponent diffusion coefficients are usually measured by creating concentration gradients in a diffusion column and then monitoring the changes in a concentration-dependent property along the column as a function of time.[3,44-51] Suitable properties include the refractive index,[44-49,52-54] conductance,[3,55] density[56] or optical absorbance.[57] The diffusion coefficients are then evaluated by fitting mathematical solutions of the multicomponent diffusion equations to the measurements. Because these solutions contain the diffusion coefficents as non-linear parameters, the determination of the multicomponent diffusivities by this procedure is difficult.[58] Consequently, D_{ik} data are scarce compared to the abundant, more easily analyzed binary data.

In this chapter, a new procedure is developed which simplifies the analysis of multicomponent diffusion experiments to the equivalent of well understood binary diffusion experiments. The idea is to treat linear combinations of measurements from two experiments run at the same final composition but with different initial

concentration gradients as simple binary data. Certain combinations will diagonalize[59,60] the multicomponent diffusion equations and yield time-invariant, pseudo-binary diffusion coefficients, the eigenvalues of D. It will be shown that the coefficients that were used to form the linear combinations define the matrix that diagonalizes D and that D is easily reconstructed by matrix manipulation.

To test the proposed eigenvalue analysis method, the multicomponent diffusion of NaOH + NaCl + H_2O has been determined. The measurements will be used to check recent predictions[55] that aqueous hydroxides diffuse faster in salt solutions than in pure H_2O and that diffusional flows of the hydroxides drive large coupled flows of salt.[5,44,54] The experimental diffusion coefficients will be compared with predictions from Onsager-Fuoss theory.

4.2 Eigenvalue Analysis Theory

To describe isothermal ternary diffusion, equation (2.2.10)

$$\partial C/\partial t = D\nabla^2 C$$

may be extended to give

$$\partial C_i/\partial t = \sum_{k=1}^{2} D_{ik}\nabla^2 C_k \qquad (4.2.1)$$

where C_i is the concentration of component i per mole of unit volume, t is the time, and ∇^2 denotes the Laplacian operator. Multicomponent diffusion coefficient D_{ik} measures the flux of component i produced by the concentration gradient in component k. In matrix form we have

$$\partial C/\partial t = D\nabla^2 C \qquad (4.2.2)$$

where C denotes the column vector of the two component concentrations and D is the 2x2 matrix of multicomponent diffusion coefficients.

Consider linear combinations[59,60] u_i of the component concentrations defined by

$$C_i = \sum_{k=1}^{2} A_{ik}\, u_k \qquad (4.2.3)$$

where A_{ik} are constants. By substituting C = Au into equation (4.2.2)

$$A\,(\partial u/\partial t) = DA\nabla^2 u \qquad (4.2.4)$$

and multiplying by A^{-1}, the expression

$$\partial u/\partial t = (A^{-1}DA)\,\nabla^2 u \qquad (4.2.5)$$

is obtained.

By choosing values for the A_{ik} coefficients so that the columns of A are eigenvectors of D, the transform of D is diagonal[61]

$$A^{-1}DA = \begin{pmatrix} D_1 & 0 \\ 0 & D_2 \end{pmatrix} \qquad (4.2.6)$$

Equations (4.2.5) and (4.2.6) then yield

$$\partial u/\partial t = \begin{pmatrix} D_1 & 0 \\ 0 & D_2 \end{pmatrix} \nabla^2 u \qquad (4.2.7)$$

or

$$\partial u_i/\partial t = D_i \nabla^2 u_i \qquad (4.2.8)$$

where D_i are eigenvalues of D and u_i are solutions of the binary diffusion equations.

The use of matrix reduction[59,60] to solve coupled differential equations is a well-known mathematical tool. The same technique will now be used to measure multicomponent diffusion coefficients without having to solve the multicomponent diffusion equations.

To measure multicomponent diffusion coefficients, a concentration-dependent property must be monitored along the diffusion path. Although the refractive index n,[44-49,52-54] density ρ,[56] or optical absorbance ϵ,[57] could

have been used, we have specialized our experiments to conductance measurements.[3,55] Hence for initial concentration differences $\Delta C_i(0)$ across a sharp diffusion boundary, the corresponding difference in conductance is

$$\Delta K(0) = S_1\Delta C_1(0) + S_2\Delta C_2(0) \qquad (4.2.9)$$

where S_1 and S_2 are the partial specific conductances

$$S_i = \partial K/\partial C_i \qquad (4.2.10)$$

evaluated at the final composition of the system. The fraction of $\Delta K(0)$ contributed by component i can be denoted as

$$X_i = S_i\Delta C_i(0)/\Delta K(0) \qquad (4.2.11)$$

Because D is not known before the start of the experiments, the exact conditions that will diagonalize D cannot be predicted. But by taking linear combinations of experiments with different initial conditions, measurements that correspond to arbitrary initial conditions may be obtained. If $\Delta K_i(t)/\Delta K_i(0)$ denotes normalized conductance measurements for an experiment in which the initial concentration gradient is entirely in component i ($\Delta C_j(0) = 0$), measurements corresponding to arbitrary initial conditions X_i may be obtained from

$$\Delta K(t)/\Delta K(0) = X_1 \Delta K_1(t)/\Delta K_1(0) + X_2 \Delta K_2(t)/\Delta K_2(0) \quad (4.2.12)$$

By writing

$$\Delta K_1(0) = S_1 \Delta C_1(0) \quad (4.2.13)$$

$$\Delta K_2(0) = S_2 \Delta C_2(0) \quad (4.2.14)$$

and using $X_2 = 1 - X_1$, the expression

$$\Delta K(t)/\Delta K(0) = X_1 \Delta K_1(t)/(S_1 \Delta C_1(0)) + (1-X_1)\Delta K_2(t)/(S_2 \Delta C_2(0)) \quad (4.2.15)$$

can be written.

By analogy with equation (3.2.10), apparent binary diffusion coefficient $D_a(\overline{t})$ may be calculated from

$$D_a\left[\frac{t'+t''}{2}\right] = -\frac{a^2}{\pi^2} \frac{\ln(\Delta K(t'')/\Delta K(0)) - \ln(\Delta K(t')/\Delta K(0))}{t''-t'} \quad (4.2.16)$$

and equation (4.2.15). Usually the apparent binary diffusion coefficients D_a obtained by this method will be time dependent.[44,47,55,62,62] For example, consider an experiment with gradients in both components, with solute 1 diffusing faster than solute 2. Initially values of D_a will be large but will decrease as the gradient in solute 1 disappears and the diffusion of solute 2 predominates. But

if experiments are run with initial conditions $X_i^{(k)}$ such that the column vector of initial concentration differences $\Delta C^{(k)}(0)$ is an eigenvector of D, then

$$D \begin{bmatrix} \Delta C_1^{(k)}(0) \\ \Delta C_2^{(k)}(0) \end{bmatrix} = D_k \begin{bmatrix} \Delta C_1^{(k)}(0) \\ \Delta C_2^{(k)}(0) \end{bmatrix} \qquad (4.2.17)$$

and one can write

$$\partial C_i^{(k)}/\partial t = D_k \nabla^2 C_i^{(k)} \qquad (4.2.18)$$

or

$$\partial K^{(k)}/\partial t = D_k \nabla^2 K^{(k)} \qquad (4.2.19)$$

As a result, the experiment behaves as a simple binary diffusion experiment with a time-variant pseudo-binary differential coefficient equal to eigenvalue D_k.

To find the correct initial conditions, the standard deviations of the apparent diffusion coefficients may be determined as a function of X_1.

$$\sigma_D = [(N-1)^{-1} \sum_{i=1}^{N} (D_a(t_i) - \bar{D}_a)^2]^{1/2} \qquad (4.2.20)$$

$$\bar{D}_a = N^{-1} \sum_{i=1}^{N} D_a(t_i) \qquad (4.2.21)$$

Minima in σ_D will be found at $X_1^{(1)}$ and $X_1^{(2)}$. At these two values of X_i, the apparent diffusion coefficients will be essentially constant over the duration of the run. The two eigenvalues D_1 and D_2 are given by the mean values of D_a at $X_1^{(1)}$ and $X_1^{(2)}$ respectively.

Once values of $X_i^{(k)}$ and D_k are established, the multicomponent diffusion coefficients are found by using

$$A_{ik} = X_i^{(k)}/S_i \qquad (4.2.22)$$

Since $X_1 + X_2 = 1$, we have

$$\mathbf{A} = \begin{bmatrix} X_1^{(1)}/S_1 & X_1^{(2)}/S_1 \\ (1-X_1^{(1)})/S_2 & (1-X_1^{(2)})/S_2 \end{bmatrix} \qquad (4.2.23)$$

The inverse transformation gives

$$\begin{bmatrix} D_{11} & D_{12} \\ D_{21} & D_{22} \end{bmatrix} = \mathbf{A}^{-1} \begin{bmatrix} D_1 & 0 \\ 0 & D_2 \end{bmatrix} \mathbf{A} \qquad (4.2.24)$$

4.3 Experimental Procedure

Ternary diffusion coefficients of dilute aqueous NaOH + NaCl mixtures were measured at 25°C using a modified version[3] of the Harned conductimetric technique.[4] At each final cell composition that was studied, paired experiments were run with different initial conditions, one with the gradient entirely in NaOH and one with the gradient

entirely in NaCl. Initial concentration differences across the diffusion boundary were 0.05-0.20 mol dm^{-3}. Cell constants were obtained by calibration with 0.1 mol dm^{-3} KCl.[2f] Values of S_1 and S_2 were determined by using an auxiliary conductance cell. Details of the cell and procedure can be found in Sections 3.2 and 3.3.

Reagent grade NaCl was dried at 140°C and used without further purification. The salt component of the solutions was added by weight. The sodium hydroxide component was prepared by dilution of highly pure saturated solutions. Winkler analyses[15,19,20a] indicated that the hydroxide solutions contained less than 0.05% carbonate based on total alkali. NaOH and NaCl concentrations were determined by potentiometric titration against potassium hydrogen phthalate and silver nitrate respectively. Solutions were made up from twice-distilled, deionized water.

4.4 Results and Discussion

4.4.1 Measured Diffusion Coefficients

Ternary diffusion coefficients for NaOH(C_1) + NaCl(C_2) + H_2O were measured at a total electrolyte concentration of 0.02 mol dm^{-3} for C_1:C_2 ratios of 1:3, 1:1, and 3:1. The results are given in Table 4.4.1. Each paired ternary experiment was performed in triplicate at each of the compositions studied. The precision of the reported D_{ik} values is quoted as ± two standard deviations.

TABLE 4.4.1

Observed and Predicted Ternary Diffusion Coefficients[a] for NaOH(1) + NaCl(2) + H_2O at 25°C

C_1[b]	C_2[b]	D_{11}[b]	D_{12}[b]	D_{21}[b]	D_{22}[b]
5.0	15.0	3.72±0.02 (3.70)	-0.38±0.04 (-0.23)	-1.34±0.13 (-1.29)	1.76±0.03 (1.71)
10.0	10.0	2.95±0.19 (2.93)	-0.33±0.07 (-0.37)	-0.71±0.21 (-0.71)	1.70±0.10 (1.82)
15.0	5.0	2.42±0.07 (2.39)	-0.52±0.01 (-0.47)	-0.31±0.10 (-0.30)	1.90±0.01 (1.89)

[a] Predicted values in parentheses

[b] Units: C_i in 10^{-3} mol dm^{-3}; D_{ik} in 10^{-9} m^2 s^{-1}

Typical results for a pair of experiments at final cell composition of C_1 = 0.0150 and C_2 = 0.0050 mol dm^{-3} are shown in Figures 4.4.1 and 4.4.2. In Figure 4.4.1, apparent binary diffusion coefficients are plotted against t for various initial conditions. For the experiment with the initial concentration gradient entirely in NaCl (X_1 = 0), 0.32 mL of solution containing 0.015 mol dm^{-3} NaOH and 0.0712 mol dm^{-3} NaCl was injected into a cell filled with solution containing 0.015 mol dm^{-3} NaOH and 0.001 mol dm^{-3} NaCl. For the experiment with the initial gradient in NaOH (X_1 = 1), 0.32 mL of solution containing 0.254 mol dm^{-3} NaOH and 0.005 mol dm^{-3} NaCl was injected into the same cell filled with 0.001 mol dm^{-3} NaOH and 0.005 mol dm^{-3} NaCl. The curves shown for X_1 = 0.4, 0.64, 0.80, 1.15, 1.21 and 1.25 were obtained by analysis of linear combinations of data from the two experiments run with X_1 = 0.00 and X_1 = 1.00.

At X_1 = 0 or 1 (gradients entirely in NaCl or NaOH respectively), the apparent diffusion coefficients vary significantly with time. But at X_1 = 0.6 or 1.2, the D_a values remain essentially constant for the duration of the experiment. The particular initial conditions that diagonalize the D matrix and yield these time-invariant diffusion coefficients were obtained by calculating the standard deviation of D_a as a function of X_1 and locating the minima in the σ_D vs X_1 plot (Figure 4.4.2). Minima were found at $X_1^{(1)}$ = 1.21 and $X_1^{(2)}$ = 0.64. From the D_a

FIGURE 4.4.1: Apparent Binary Diffusion Coefficients of NaOH(1) + NaCl(2) + H_2O for C_1 = 0.015 mol dm^{-3} and C_2 = 0.005 mol dm^{-3} for Selected Initial Conditions.

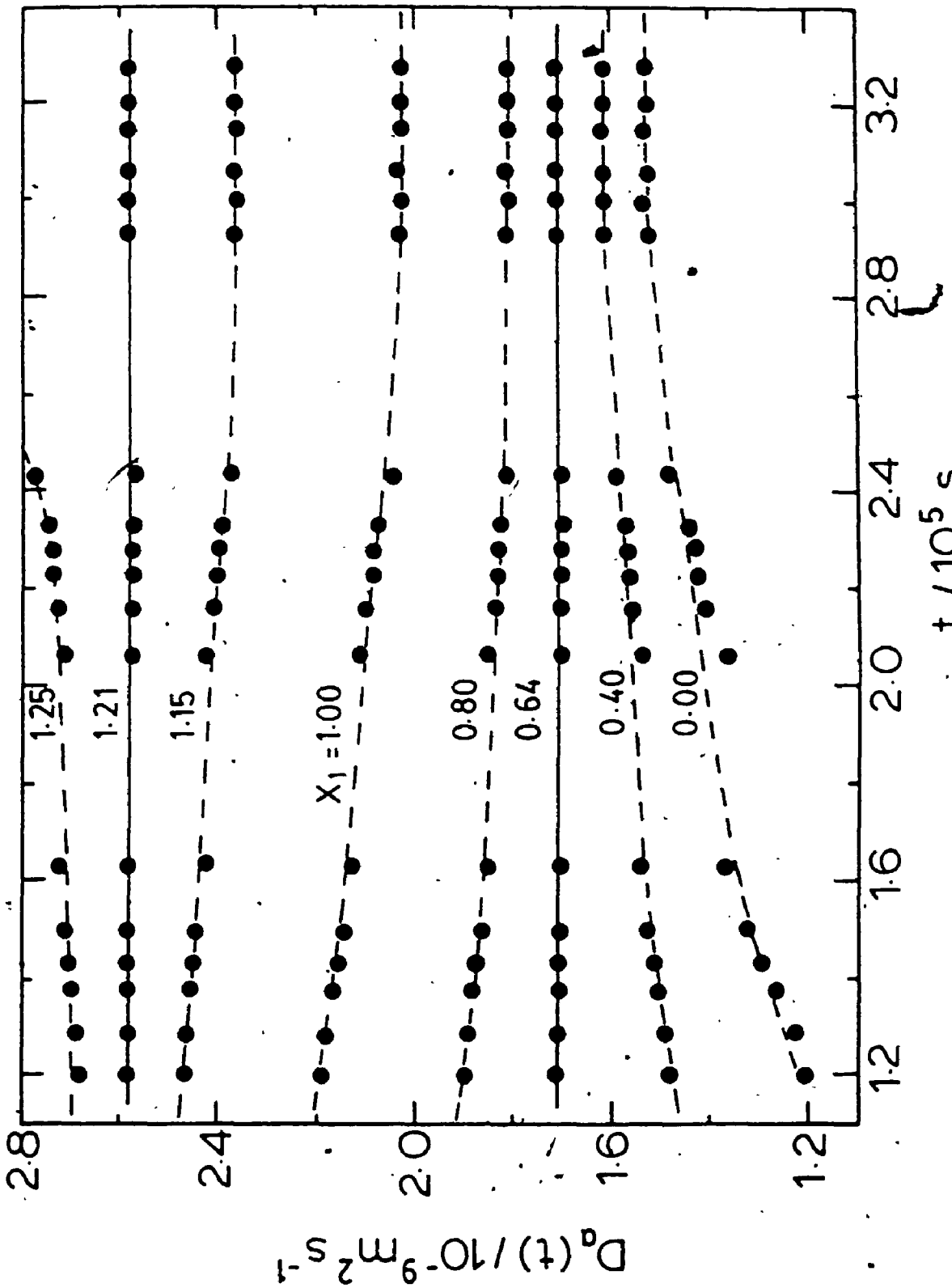
$D_a(t) / 10^{-9} m^2 s^{-1}$
2.8
2.4
2.0
1.6
1.2
1.2
1.6
2.0
2.4
2.8
3.2
$t / 10^5$ s
1.25
1.21
1.15
$x_1 = 1.00$
0.80
0.64
0.40
0.00

FIGURE 4.4.2: Standard Deviation of the Apparent Diffusion Coefficients of NaOH(1) + NaCl(2) + H_2O for C_1 = 0.015 mol dm^{-3} and C_2 = 0.005 mol dm^{-3}.

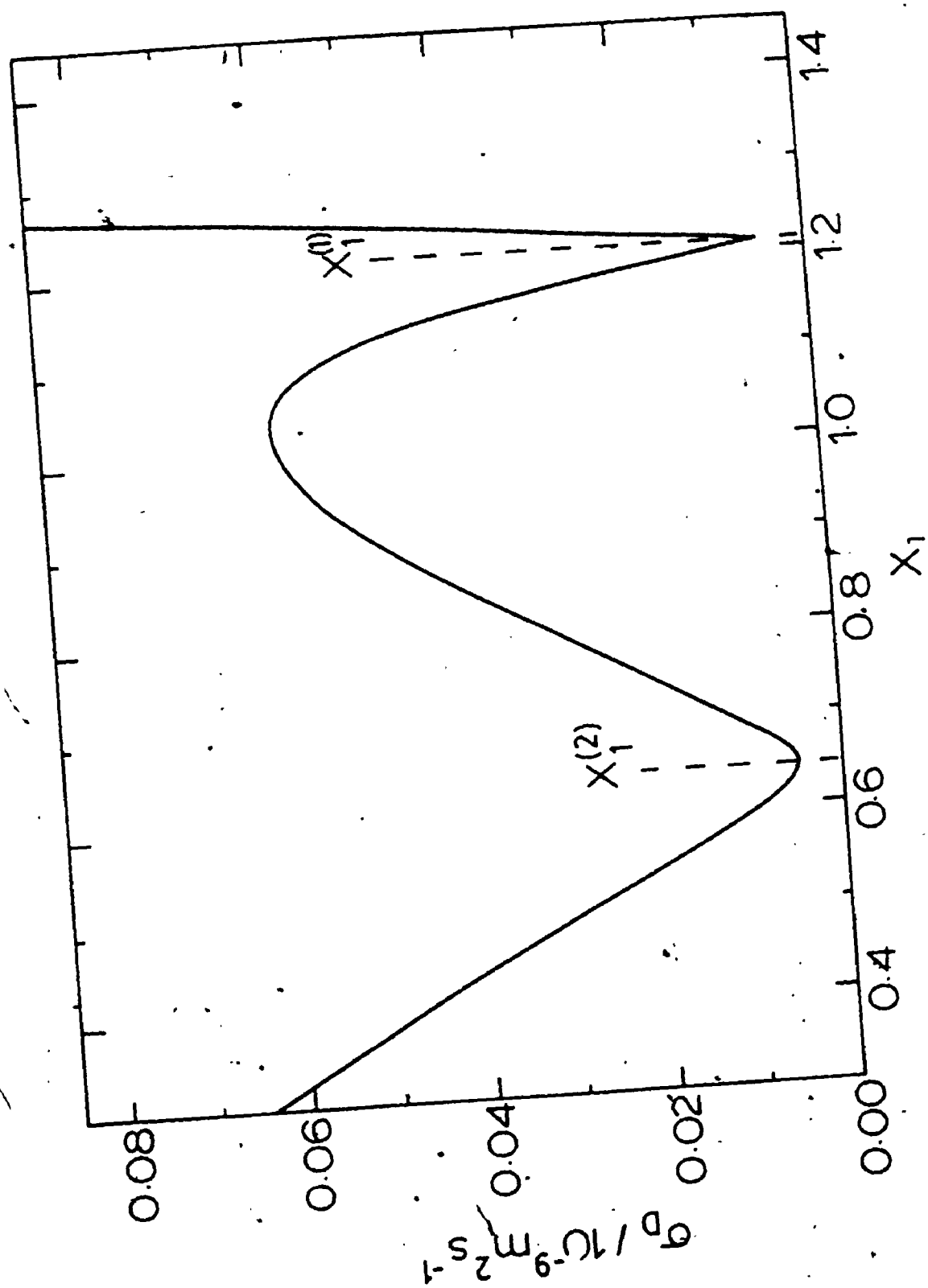
$\sigma_D / 10^{-9} m^2 s^{-1}$
0.08
0.06
0.04
0.02
0.00
0.4
0.6
0.8
1.0
1.2
1.4
x_1
$x_1^{(1)}$
$x_1^{(2)}$

values evaluated at these two X_1 values, eigenvalues $D_1 = 2.58 \times 10^{-9}$ and $D_2 = 1.71 \times 10^{-9}$ m^2 s^{-1} were obtained. Table 4.4.2 summarizes the values for S_1/S_2, $X_1(1)$, $X_1(2)$, D_1 and D_2 for each of the compositions studied.

4.4.2 Predicted Diffusion Coefficients

Diffusion in aqueous NaOH + NaCl solutions involves the transport of three solute species (Na^+, OH^-, Cl^-). The restriction of zero electric current provides that the flux of the positively charged ions must balance the flux of the negatively charged ions. Therefore only two flows are independent ($N = 2$) and the diffusion properties are ternary.

Numbering the components 1 = NaOH, 2 = NaCl and constitutent ions 1 = OH^-, 2 = Cl^- and 3 = Na^+ defines

$$\nu = \begin{pmatrix} 1 & 0 \\ 0 & 1 \\ 1 & 1 \end{pmatrix} \qquad (4.4.1)$$

For the ion transport coefficients we have

$$\ell' = \begin{pmatrix} \ell_{11} & \ell_{12} & \ell_{13} \\ \ell_{21} & \ell_{22} & \ell_{23} \\ \ell_{31} & \ell_{32} & \ell_{33} \end{pmatrix} \qquad (4.4.2)$$

TABLE 4.4.2

Parameters Used to Calculate Experimental Diffusion Coefficients for NaOH(1) + NaCl(2) + H_2O at 25°C

C_1[a]	C_2[a]	S_1/S_2	$X_1(1)$	$X_1(2)$	D_1[a]	D_2[a]
5.0	15.0	2.12	1.42±0.05	0.23±0.03	3.91±0.02	1.58±0.02
10.0	10.0	1.90	1.36±0.09	0.31±0.06	3.12±0.23	1.54±0.06
15.0	5.0	2.29	1.23±0.05	0.62±0.04	2.64±0.11	1.69±0.03

[a] Units: C_i in 10^{-3} mol dm^{-3}; D_i in 10^{-9} m^2 s^{-1}

The ℓ_{ik} coefficients can be expressed as the sum of the limiting coefficient ℓ°_{ik}, the electrophoretic term $\ell^{'}_{ik}$ and the relaxation term $\ell^{''}_{ik}$ [3]

$$\ell_{ik} = \ell^{\circ}_{ik} + \ell^{'}_{ik} + \ell^{''}_{ik} \qquad (4.4.3)$$

where $\ell^{\circ}_{ik} = \delta_{ik}c_iD^{\circ}_i/RT$. Due to the complexity of the expressions for $\ell^{'}_{ik}$ and $\ell^{''}_{ik}$,[3,64,65] they are not given here. It should be noted that with the inclusion of the $\ell^{'}_{ik}$ and $\ell^{''}_{ik}$ terms, ℓ is no longer diagonal. The origin of the relaxation effect can be traced to the asymmetry of the ion atmosphere surrounding the ion. As an ion moves through solution, it is surrounded by a sheath of water molecules, known as the ion atmosphere. With different ions moving at different velocities, the atmosphere scatters in one direction and collects in the other direction. Because the formation of the ion atmosphere is not instantaneous, the atmosphere will be deformed and the position of the ion will no longer coincide with the centre of the atmosphere. Consequently, an electrostatic force will be exerted on the central ion. In contrast, for binary diffusion, the relaxation effect is negligible. The ions move at the same speed and the atmosphere remains symmetrical. The origin of the electrophoretic effect has been discussed in Section 2.3.

Equations (2.4.17), and (4.4.1)-(4.4.3) then give the Onsager coefficients for the neutral electrolyte components.

The concentrations of the constituent ions are given in terms of the concentrations of components NaOH(1) and NaCl(2).

$$c_1(OH^-) = C_1 \qquad (4.4.4)$$

$$c_2(Cl^-) = C_2 \qquad (4.4.5)$$

$$c_3(Na^+) = C_1 + C_2 \qquad (4.4.6)$$

The chemical potentials of the two components are given by

$$\mu_1 = \mu_1^\circ + RT\ln[C_1(C_1+C_2)y_{\pm 1}^2] \qquad (4.4.7)$$

$$\mu_2 = \mu_2^\circ + RT\ln[C_2(C_1+C_2)y_{\pm 2}^2] \qquad (4.4.8)$$

Mean ionic activity coefficients (on the molar concentration scale) were evaluated using Guggenheim's expression for two 1:1 electrolytes with a common ion.[21]

$$\ln y_{\pm 1} = -\frac{\alpha(C_1+C_2)^{1/2}}{1 + (C_1+C_2)^{1/2}} + \beta_1 C_1 + \beta_2 C_2 + \beta_1(C_1+C_2) \qquad (4.4.9)$$

where α is the Debye-Huckel constant and β_1 are small empirical constants which allow for ionic interactions.

Differentiation of equations (4.4.7) and (4.4.8) leads to the following expressions

$$\mu_{11}/RT = \frac{1}{C_1} + \frac{1}{(C_1+C_2)} + 2\,\partial \ln y_{\pm 1}/\partial C_1 \qquad (4.4.10)$$

$$\mu_{12}/RT = \frac{1}{(C_1+C_2)} + 2\,\partial \ln y_{\pm 1}/\partial C_2 \qquad (4.4.11)$$

$$\mu_{21}/RT = \frac{1}{(C_1+C_2)} + 2\,\partial \ln y_{\pm 2}/\partial C_1 \qquad (4.4.12)$$

$$\mu_{22}/RT = \frac{1}{C_2} + \frac{1}{(C_1+C_2)} + 2\,\partial \ln y_{\pm 2}/\partial C_2 \qquad (4.4.13)$$

From the derivatives $\mu_{mk} = \partial \mu_m/\partial C_k$ (equations (4.4.10)-(4.4.13)) and the component Onsager coefficients, the diffusion coefficients are obtained using equation (2.4.3)

$$D_{11} = L_{11}\mu_{11} + L_{12}\mu_{21} \qquad (4.4.14)$$

$$D_{12} = L_{11}\mu_{12} + L_{12}\mu_{22} \qquad (4.4.15)$$

$$D_{21} = L_{21}\mu_{11} + L_{22}\mu_{21} \qquad (4.4.16)$$

$$D_{22} = L_{21}\mu_{12} + L_{22}\mu_{22} \qquad (4.4.17)$$

Values of the parameters used in the calculations are listed in Table 4.4.3.

In Table 4.4.1, the experimental diffusion coefficients are compared with predicted values. Experimental L_{ik} values obtained from measured values of D_{ik} and calculated values of μ_{mk} by using the inverse of equation (2.4.3)

$$L = D\mu^{-1} \qquad (4.4.18)$$

are compared with theoretical predictions in Table 4.4.4. Agreement is very good. The observed values of the L_{ik} coefficients are consistent with the Onsager reciprocal relation $L_{12} = L_{21}$.[66,67]

Measured values of D_{11}, the ternary diffusivity of the NaOH component, range from 2.42×10^{-9} to 3.72×10^{-9} $m^2\ s^{-1}$, increasing as the solution becomes richer in salt. At similar concentrations, the binary diffusivity[68] of aqueous NaOH is much smaller, about 1.99×10^{-9} $m^2\ s^{-1}$. In binary NaOH solutions, OH^- ions are constrained by electroneutrality to diffuse at the same rate as the less mobile Na^+ ions. In the ternary electrolyte solutions, OH^- can diffuse much faster. Electroneutrality is maintained because the induced electric field drives countercurrent flow of Cl^- ions. Hence coupled transport of Cl^- ions can explain both the enhanced diffusivity of the NaOH component and the negative value for D_{21}. Similar behaviour was reported for HCl + NaCl + H_2O and other acid-containing

TABLE 4.4.3

Molar Ionic Conductances and Other Parameters[a] Used to Calculate Theoretical Values for the Transport Coefficients for NaOH(1) + NaCl(2) + H_2O at 25°C

Electrolyte	Λ°_{+m}[b]	Λ°_{-m}[b]	β[b]
NaOH	50.10	198.3	0.08[c]
NaCl	50.10	76.35	0.16[d]

[a] Ion size parameter[3] a = 4x 10^{-10} m.

[b] Units: $\Lambda^{\circ}_{+,-m}$ in 10^{-4} m^2 S mol^{-1}; β in dm^{-3} mol

[c] Ref. 68

[d] Ref. 27

TABLE 4.4.4

Comparison of Observed and Predicted L_{ik} Coefficients[a] for NaOH(1) + NaCl(2) + H_2O at 25°C

C_1[b]	C_2[b]	RTL_{11}[b]	RTL_{12}[b]	RTL_{21}[b]	RTL_{22}[b]
5.0	15.0	1.69±0.02 (1.67)	-0.94±0.04 (-0.87)	-0.90±0 (-0.87)	1.94±0.05 (1.89)
10.0	10.0	2.18±0.16 (2.33)	-0.94±0.09 (-0.97)	-0.94±0.18 (-0.97)	1.47±0.12 (1.55)
15.0	5.0	2.27±0.09 (2.41)	-0.65±0.05 (-0.63)	-0.64±0.10 (-0.63)	0.89±0.02 (0.89)

[a] Predicted values in parentheses

[b] Units: C_i in 10^{-3} mol dm^{-3}; L_{ik} in 10^{-9} mol m^{-1} s^{-1}

mixed electrolytes.[44,54,55] In these cases, the electric field induced by the faster moving ion (the proton) generates counterflow of cation.

Since the difference in mobilities between Na^+ and Cl^- is much less than the corresponding difference for NaOH, NaCl gradients generate relatively weak electric fields. Consequently, D_{12} values are small. As a result, D_{22}, the ternary diffusivity of the NaCl component is much closer to its binary diffusivity[21] (1.79 x 10^{-9} vs 1.55 x 10^{-9} m^2 s^{-1} respectively).

Because the experimental diffusion coefficients evaluated by the eigenvalue analysis technique agree quite well with theoretical predictions and because the Onsager reciprocal relation was satisfied, the eigenvalue method of analysis appears to be reliable. As an additional check, experimental diffusion coefficients for NaOH + NaCl + H_2O mixtures were evaluated by a previously reported non-linear least squares procedure.[69] The results are listed in Table 4.4.5. Comparison of Tables 4.4.1 and 4.4.5 indicates that the eigenvalue and non-linear least squares procedure give essentially identical results. In practice, however, the eigenvalue analysis procedure is much easier to use. The problem of finding four minima in four dimensions is reduced to finding two minima in one dimension.

Because of the success of the eigenvalue method for ternary systems, it is a logical extension to apply the eigenvalue procedure to the determination of quaternary

TABLE 4.4.5

Experimental Diffusion Coefficients for NaOH(1) + NaCl(2) + H_2O at 25°C Determined by Non-Linear Least Squares

C_1[a]	C_2[a]	D_{11}[a]	D_{12}[a]	D_{21}[a]	D_{22}[a]
5.0	15.0	3.77±0.15	-0.27±0.04	-1.35±0.19	1.72±0.05
10.0	10.0	3.02±0.02	-0.35±0.08	-0.75±0.14	1.75±0.08
15.0	5.0	2.45±0.07	-0.55±0.08	-0.33±0.08	1.93±0.02

[a] Units: C_i in 10^{-3} mol dm^{-3}; D_{ik} in 10^{-9} m^2 s^{-1}

diffusion coefficients.[58] For these systems, the non-linear least squares method would require simultaneous optimization of nine parameters. Application of the eigenvalue technique would reduce the problem to finding three minima in two dimensions, a much easier task.

4.5 Summary and Conclusions

If linear combinations of data from experiments run at the same composition but with different initial conditions are analyzed as binary data, certain combinations can be found that transform the multicomponent diffusion coefficient matrix, D, to diagonal form. The pseudo-binary diffusion coefficients that are determined from these combinations of data give the eigenvalues of the multicomponent diffusion coefficient matrix. Because the coefficients used to take the linear combinations define the matrix that diagonalized D, D can be recovered by the inverse transformation. To test the eigenvalue procedure, ternary diffusion coefficients for the system NaOH + NaCl + H_2O were determined. Measurements show that NaOH diffuses much faster in salt solutions than in pure water and that large coupled flows of NaCl are produced. Agreement between measured and predicted transport coefficients is very good.

CHAPTER FIVE

DIFFUSION OF METAL SULFATES IN AQUEOUS ACIDIC MEDIA: COPPER SULFATE + SULFURIC ACID + WATER MIXTURES

5.1 Introduction

Aqueous copper sulfate + sulfuric acid mixtures are used in electrorefining and electroplating of copper. Typical solution compositions[70] range from 0.6-0.9 mol dm^{-3} $CuSO_4$, 1.8-2.5 mol dm^{-3} H_2SO_4 for electrorefining and 1.2-1.6 mol dm^{-3} $CuSO_4$, 0.2-0.5 mol dm^{-3} H_2SO_4 for electroplating. To fully understand mass transport in these processes, accurate diffusion data are required.

In previous studies, diffusion of $CuSO_4$ in aqueous H_2SO_4 solutions was treated as a binary process by using a pseudo-binary Fick equation

$$-J_1 = D_{11}^a \nabla C_1 \qquad (5.1.1)$$

where J_1 is the flux of the $CuSO_4$ component, D_{11}^a is the apparent binary diffusion coefficient and ∇C_1 is the $CuSO_4$ concentration gradient. Cole and Gordon[71] measured the diffusion of $CuSO_4$ in $H_2SO_4 + H_2O$ using a McBain cell (which is essentially one-half of a Stokes diaphragm cell). They reported that the diffusivity of $CuSO_4$ fell as the acid concentration of the solution was raised. More

recently, Awakura et al.,[72] using a modified Lamm scale method, found that the diffusivity of $CuSO_4$ in aqueous sulfuric acid solutions was greater than the salt's binary diffusivity in pure H_2O. Additionally, they reported that if the acid concentration was raised above 1.5 mol dm^{-3}, the $CuSO_4$ diffusivity decreased. The lowered diffusivity was thought to be the result of increased solution viscosity.[72]

Diffusion in aqueous $CuSO_4$ + H_2SO_4 mixtures involves the transport of four solute species (Cu^{2+}, SO_4^{2-}, H^+, HSO_4^-) with two constraints: electroneutrality and local chemical equilibrium of the bisulfate dissociation reaction. Hence two independent flows exist, and diffusion of aqueous $CuSO_4$ + H_2SO_4 is a ternary process described by

$$-J_1 = D_{11}\nabla C_1 + D_{12}\nabla C_2 \qquad (5.1.2)$$

$$-J_2 = D_{21}\nabla C_1 + D_{22}\nabla C_2 \qquad (5.1.3)$$

This work was undertaken to determine ternary diffusivities for the $CuSO_4$ + H_2SO_4 + H_2O system. Conductimetric and diaphragm cell techniques were used. In order to study the effects of the bisulfate dissociation on diffusion, measurements were extended to low concentrations. The relationship between the apparent (D_{11}^a) and true (D_{11}) diffusivities will be discussed. It

will be shown that the measured apparent diffusivities of copper sulfate can be 1 to 8% lower than the salt's true diffusivity.

5.2 Stokes Diaphragm Technique

In the Stokes diaphragm cell technique,[1,2a] diffusion is followed by measuring changes in concentrations after solute diffuses between two solution compartments through the pores of a sintered-glass diaphragm.

For binary diffusion of a single solute, the rates of change of the solute concentration across the diaphragm at time t can be expressed as

$$dC_U/dt = J(t)A/V_U \qquad (5.2.1)$$

$$dC_L/dt = -J(t)A/V_L \qquad (5.2.2)$$

where C_U, V_U and C_L, V_L are the solute concentration and volume of the upper and lower compartments respectively. A is the cross-sectional area of the diaphragm. The net flow out of the diaphragm is given by

$$d(C_L-C_U)/dt = -J(t)A\left(\frac{1}{V_L}+\frac{1}{V_U}\right) \qquad (5.2.3)$$

Since $$J = -D\, dC/dx \qquad (5.2.4)$$

Then $$J(t) = -\bar{D}(C_L-C_U)/\ell \qquad (5.2.5)$$

where $\bar{D}$ is the average diffusion coefficient over the concentration range C_L-C_U. ℓ is the effective thickness of the diaphragm (see Figure 5.2.1).

Combination of equations (5.2.3) and (5.2.5) gives

$$\frac{1}{(C_L-C_U)}\, d(C_L-C_U)/dt = \bar{D}\,\frac{A}{\ell}\left(\frac{1}{V_L}+\frac{1}{V_U}\right) \qquad (5.2.6)$$

or

$$d\ell n(C_L-C_U)/dt = \bar{D}\beta \qquad (5.2.7)$$

where β is the cell constant defined by

$$\beta = \frac{A}{\ell}\left(\frac{1}{V_L}+\frac{1}{V_U}\right) \qquad (5.2.8)$$

Integrating equation(5.2.7) between the limits

$$C_L = C_1,\ C_U = C_2;\quad t = 0 \qquad (5.2.9)$$

$$C_L = C_3,\ C_U = C_4;\quad t = t_f \qquad (5.2.10)$$

yields

$$\ell n[(C_1-C_2)/(C_3-C_4)] = \bar{D}\beta t_f \qquad (5.2.11)$$

where t_f is the experiment duration.

FIGURE 5.2.1: Stokes Diaphragm Cell

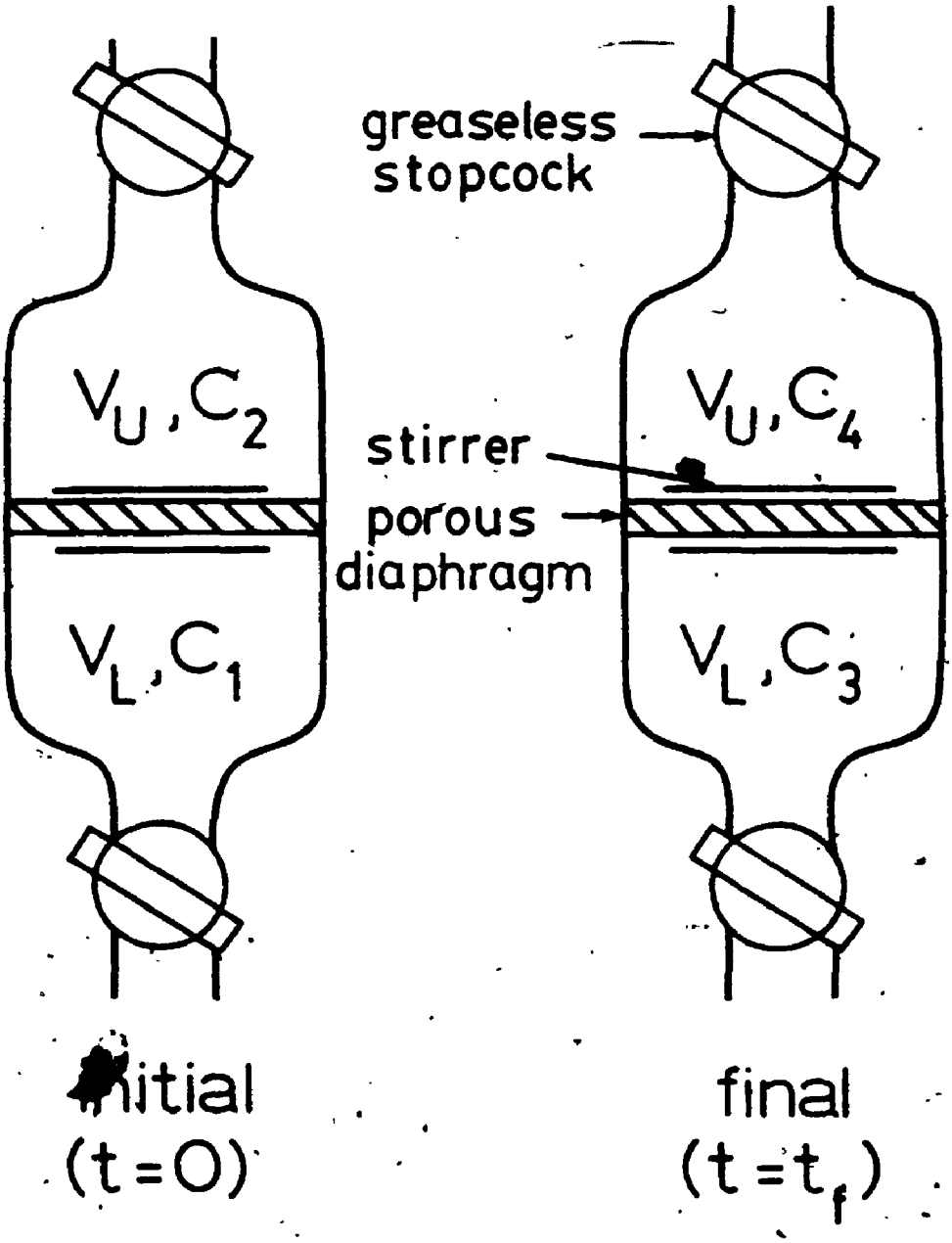
greaseless
stopcock
V_U, C_2
V_U, C_4
stirrer
porous
diaphragm
V_L, C_1
V_L, C_3
initial
(t=0)
final
($t = t_f$)

If the concentration differences are written as $\Delta C(0) = C_1 - C_2$ and $\Delta C(t_f) = C_3 - C_4$, the binary behaviour of a diaphragm cell can be expressed as

$$\bar{D} = \frac{1}{\beta t_f} \ln(\Delta C(0)/\Delta C(t_f)) \qquad (5.2.12)$$

Multicomponent integral diffusion coefficients were determined by the matrix method developed by Kosanovich and Cullinan.[51,73] Equation (5.2.12) can be rearranged and rewritten as

$$\Delta C(0)(\Delta C(t_f))^{-1} = \exp(\bar{D}\beta t_f) \qquad (5.2.13)$$

where $\bar{D}$ is the NxN diffusion coefficient matrix. $\Delta C(0)$ and $\Delta C(t_f)$ are NxN matrices which relate the initial and final concentration differences across the diaphragm at time βt_f. If **X** is defined as

$$\mathbf{X} = \Delta C(0)(\Delta C(t_f))^{-1} \qquad (5.2.14)$$

the multicomponent diffusion coefficients are given by

$$\bar{D} = P \begin{bmatrix} \ln X_1 & & \\ & \ln X_2 & \\ & & \ddots \end{bmatrix} P^{-1}/\beta t_f \qquad (5.2.15)$$

where X_i are the eigenvalues of **X** and the columns of **P** are eigenvectors of **X**.

5.3 Experimental Procedure.

A modified version[3] of Harned's conductimetric technique[4] was used to measure ternary diffusion in $CuSO_4(C_1) + H_2SO_4(C_2) + H_2O$ mixtures for compositions $C_1 + C_2$ up to 0.5 mol dm^{-3}. Electrical resistances were measured using a General Radio 1689 automatic a.c. bridge. The bridge was interfaced with a Hewlett Packard 3488A switch unit and a Hewlett Packard model 216 computer for data acquisition and analysis. Automation of the Harned experiment reduces the possibility of cell convection by electrical heating during the time-consuming manual bridge balancing. Also, computer acquisition of data eliminates overnight gaps in conductance readings taken manually.

Stokes diaphragm cells[1,2a] were used to measure diffusion coefficients for concentrated solutions which were similar in concentration to typical plating baths. The cells were constructed from Pyrex with fine-porosity sintered-glass diaphragms (pore diameter 5×10^{-6} m). Each compartment (approximate volume 0.030 dm^{-3}) was fitted with a greaseless teflon stopcock and magnetically stirred at 60 rpm by glass enclosed iron wire stirrers. Cells were calibrated at frequent intervals with aqueous potassium chloride[1] (0.5 mol dm^{-3}). Concentrations of the chloride solutions from the calibration runs were determined by

potentiometric titration against silver nitrate. Cell constants were reproducible to 0.2%.

The run is started by filling both compartments with solutions of known concentrations. The cell is placed in a thermostatted bath and run for about two hours to set up steady state conditions in the diaphragm. The solutions are then replaced, the cell returned to the bath and left stirring for three to four days. At the end of the run, the solutions are analyzed to determine the rate of diffusion through the diaphragm.

Ternary integral diffusion coefficients were determined by the matrix method developed by Kosanovich and Cullinan.[51,73] Two paired diaphragm cell runs A and B of identical duration were carried out with different initial concentration differences ($\Delta C^A(0)$, $\Delta C^B(0)$) across the diaphragm. In this case, X is given by

$$X = \begin{bmatrix} \Delta C_1^A(0) & \Delta C_1^B(0) \\ \Delta C_2^A(0) & \Delta C_2^B(0) \end{bmatrix} \cdot \begin{bmatrix} \Delta C_1^A(t_f) & \Delta C_1^B(t_f) \\ \Delta C_2^A(t_f) & \Delta C_2^B(t_f) \end{bmatrix}^{-1} \quad (5.3.1)$$

Diffusion coefficients are given by equation (5.2.15).

The concentration of $CuSO_4$ (C_1) was determined by iodine-sodium thiosulfate titrations.[20b,74a] Due to possible interference from the intense blue colour of the more concentrated copper solutions, the solutions were diluted to approximately 0.050 mol dm^{-3}. Titration with

standardized NaOH gave the concentration of $H_2SO_4(C_2)$. C_1 and C_2 values were reproducible to 0.5%. Titrations were performed in triplicate.

Stock solutions of $CuSO_4$ were prepared from analytical reagent grade $CuSO_4.5\ H_2O$. Stock solutions of H_2SO_4 were prepared by dilution of concentrated reagent grade acid. Doubly distilled, deionized H_2O was used. The concentrations of the two stock solutions were determined by titration.

5.4 Results and Discussion

Ternary diffusion coefficients for $CuSO_4(C_1)$ + $SO_4(C_2)$ + H_2O mixtures were determined conductimetrically at total electrolyte concentrations of 0.01, 0.05 and 0.5 mol dm^{-3} for $C_1:C_2$ ratios of 1:3, 1:1, and 3:1. Results are shown in Table 5.4.1. Data were analyzed using a previously reported conductimetric technique.[75] Table 5.4.2 gives the results of the diaphragm cell experiments at the composition 1.2 mol dm^{-3} $CuSO_4$, 0.2 mol dm^{-3} H_2SO_4. Paired diffusion experiments were performed in triplicate at each of the concentrations studied. Precision of the data is quoted as ± two standard deviations.

Examination of Tables 5.4.1 and 5.4.2 indicates that for most compositions, the ternary diffusivity of $CuSO_4$ is larger than its binary value[76-78] at the same concentration. For example at 1.2 mol dm^{-3} $CuSO_4$,

TABLE 5.4.1

Ternary Diffusion Coefficients[a] Determined Conductimetrically for $CuSO_4$(1) + H_2SO_4(2) + H_2O at 25°C

C_1[b]	C_2[b]	D_{11}[b]	D_{12}[b]	D_{21}[b]	D_{22}[b]
0.0075	0.0025	0.73 ± 0.01 (0.68)	-0.75 ± 0.10 (-1.40)	-0.22 ± 0.04 (-0.22)	3.78 ± 0.08 (4.95)
0.0050	0.0050	0.67 ± 0.02 (0.72)	-0.51 ± 0.02 (-0.75)	-0.120 ± 0.008 (-0.303)	2.91 ± 0.01 (3.68)
0.0025	0.0075	0.689 ± 0.006 (0.728)	-0.19 ± 0.02 (-0.31)	-0.091 ± 0.006 (-0.317)	2.367 ± 0.006 (2.803)
0.0750	0.0250	0.65 ± 0.02 (0.55)	-0.44 ± 0.04 (-1.09)	-0.29 ± 0.01 (0.36)	3.07 ± 0.08 (4.17)
0.0500	0.0500	0.64 ± 0.02 (0.68)	-0.31 ± 0.02 (-0.73)	-0.27 ± 0.01 (-0.66)	2.48 ± 0.01 (3.52)
0.0250	0.0750	0.69 ± 0.04 (0.73)	-0.07 ± 0.02 (-0.34)	-0.14 ± 0.02 (-0.79)	2.10 ± 0.01 (2.74)
0.3750	0.1250	0.50 ± 0.10 (0.52)	-0.38 ± 0.02 (-0.84)	-0.13 ± 0.02 (-0.38)	2.61 ± 0.02 (3.65)
0.2500	0.2500	0.50 ± 0.06 (0.71)	-0.28 ± 0.02 (-0.73)	-0.15 ± 0.02 (-0.88)	2.30 ± 0.02 (3.52)
0.1250	0.3750	0.52 ± 0.02 (0.76)	-0.05 ± 0.04 (-0.36)	-0.18 ± 0.04 (-1.09)	2.00 ± 0.06 (2.79)

[a] Predicted values in parentheses; [b] Units: C_i in mol dm^{-3}; D_{ik} in 10^{-9} m^2 s^{-1}

TABLE 5.4.2

Ternary Diffusion Coefficients for $CuSO_4$ (1.20 mol dm^{-3}) + H_2SO_4 (0.20 mol dm^{-3}) + H_2O from Diaphragm Cell Experiments at 25°C

	D_{11}[a]	D_{12}[a]	D_{21}[a]	D_{22}[a]
Measured	0.66±0.02	-0.21±0.01	-0.10±0.01	1.87±0.07
Predicted	0.49	-0.56	-0.17	3.02

[a] Units: D_{ik} in 10^{-9} m^2 s^{-1}

0.2 mol dm^{-3} H_2SO_4, D_{11} equals 0.66 x 10^{-9} m^2 s^{-2}, nearly 40% larger than its corresponding binary value.[76-78]

When a concentration gradient in $CuSO_4$ is formed in an acidic solution, the ion association equilibrium $H^+ + SO_4^{2-} \rightleftharpoons HSO_4^-$ produces a gradient of opposite sign in the concentration of H^+ ions. As the H^+ ions diffuse down their gradient toward the $CuSO_4$-rich region, an electric field is generated to slow them down in order to maintain electroneutrality. The electric field in turn speeds up the Cu^{2+} ion in the opposite direction. Both the enhanced diffusivity of the copper sulfate component and the negative values for D_{21}, the cross coefficient that measures the flow of H_2SO_4 caused by gradients in $CuSO_4$ concentrations, are explained by this mechanism.

D_{22}, the ternary diffusivity of the H_2SO_4 component, is significantly larger than its binary value.[79] Counterflow of Cu^{2+} ions allows the H^+ ions to diffuse rapidly while still maintaining electroneutrality. Consequently, values of D_{12} are negative. At low acid concentrations, a higher portion of H^+ ions are present as a result of the increased significance of the bisulfate dissociation reaction. Hence D_{12} becomes more negative. As the $CuSO_4$:H_2SO_4 ratio increases, D_{12} vanishes because there are no Cu^{2+} ions for the H^+ ions to push. Accordingly, D_{22} falls as well.

The concentration-dependence of the D_{ik} coefficients for $CuSO_4$ + H_2SO_4 + H_2O mixtures will now be discussed.

Numbering the components, constituent ions and solute species as follows: 1 = $CuSO_4$, 2 = H_2SO_4; 1 = Cu^{2+}, 2 = H^+, 3 = SO_4^{2-}; and 1 = Cu^{2+}, 2 = H^+, 3 = SO_4^{2-} and 4 = HSO_4^- yields

$$\nu = \begin{pmatrix} 1 & 0 \\ 0 & 2 \\ 1 & 1 \end{pmatrix} \qquad (5.4.1)$$

$$\nu = \begin{pmatrix} 1 & 0 & 0 & 0 \\ 0 & 1 & 0 & 1 \\ 0 & 0 & 1 & 1 \end{pmatrix} \qquad (5.4.2)$$

ℓ can be written as

$$\ell = \begin{pmatrix} \ell_{11} & 0 & 0 & 0 \\ 0 & \ell_{22} & 0 & 0 \\ 0 & 0 & \ell_{33} & 0 \\ 0 & 0 & 0 & \ell_{44} \end{pmatrix} \qquad (5.4.3)$$

Combining equations (2.5.7), (5.4.2) and (5.4.3) yields

$$\ell = \begin{pmatrix} \ell_{11} & 0 & 0 \\ 0 & \ell_{22} + \ell_{44} & \ell_{44} \\ 0 & \ell_{44} & \ell_{33} + \ell_{44} \end{pmatrix} \qquad (5.4.4)$$

with i_{1k} given by equation (2.5.13). D_i is given by equation (3.4.2). From limiting conductances[2e,80] $D_1(Cu^{2+}) = 0.71 \times 10^{-9}$, $D_2(H^+) = 9.315 \times 10^{-9}$, $D_3(SO_4^{2-}) = 1.065 \times 10^{-9}$ and $D_4(HSO_4^-) = 1.363 \times 10^{-9}$ $m^2\ s^{-1}$.

The concentrations of the species are given by

$$c_1(Cu^{2+}) = C_1 \qquad (5.4.5)$$

$$c_2(H^+) = (B-1)C_1 + (B+1)C_2 \qquad (5.4.6)$$

$$c_3(SO_4^{2-}) = B(C_1+C_2) \qquad (5.4.7)$$

$$c_4(HSO_4^-) = (1-B)(C_1+C_2) \qquad (5.4.8)$$

where B is an abbreviation for the extent of bisulfate dissociation

$$B = c_3(SO_4^{2-})/[c_3(SO_4^{2-}) + c_4(HSO_4^-)] \qquad (5.4.9)$$

Values of B can be calculated from the equilibrium condition[81,82]

$$K_{a2} = (c_2c_3/c_4)(y_2y_3/y_4) \qquad (5.4.10)$$

$$K_{a2} = 0.0105 \text{ mol dm}^{-3} \text{ at } 25°C$$

Because activity coefficient data are not available for $CuSO_4 + H_2SO_4 + H_2O$ mixtures, the activity coefficient terms for the ions were evaluated from[27]

$$\ln y_i = -z_i^2 \alpha I^{1/2}/(1 + I^{1/2}) \qquad (5.4.11)$$

where z_i is the valence of species i and I, the ionic strength, equals $2(1+B)C_1 + (1+2B)C_2$. After some algebraic manipulation of equations (2.5.8), (5.4.1) and (5.4.4), the L_{ik} coefficients are obtained

$$L_{11} = [4(b+d) + c]/[4b(a+c) + 4d(a-d) + ac] \qquad (5.4.12)$$

$$L_{12} = L_{21} = [-(2d+c)]/[4b(a+c) + 4d(a-d) + ac] \qquad (5.4.13)$$

$$L_{22} = [a+c]/[4b(a+c) + 4d(a-d) + ac] \qquad (5.4.14)$$

where

$$a = 1/\ell_{11} \qquad (5.4.15)$$

$$b = [\ell_{33}+\ell_{44}]/[\ell_{22}(\ell_{33}+\ell_{44}) + \ell_{33}\ell_{44}] \qquad (5.4.16)$$

$$c = [\ell_{22}+\ell_{44}]/[\ell_{22}(\ell_{33}+\ell_{44}) + \ell_{33}\ell_{44}] \qquad (5.4.17)$$

$$d = [-\ell_{44}]/[\ell_{22}(\ell_{33}+\ell_{44}) + \ell_{33}\ell_{44}] \qquad (5.4.18)$$

Values for $\partial\mu_m/\partial C_k$ are obtained by differentiation of expressions for the chemical potentials of the solute components

$$\mu_1 = \mu_1^\circ + RT\ln[c_1 c_3 y_1 y_3] \qquad (5.4.19)$$

$$\mu_2 = \mu_2^\circ + RT\ln[c_2^2 c_3 y_2^2 y_3] \qquad (5.4.20)$$

along with equations (5.4.5)-(5.4.11). Ternary diffusion coefficients are then obtained from equations (4.4.14)-(4.4.17).

In Figures 5.4.1 and 5.4.2, experimental and theoretical diffusion coefficients are compared. The coefficients are plotted against $C_1/(C_1+C_2)$, the fraction of the $CuSO_4$ component in the $CuSO_4 + H_2SO_4 + H_2O$ mixture. Although the agreement is not quantitative, the signs, magnitudes and trends with concentration are correctly predicted. In view of the dilute solution approximation made in the analysis, agreement is found to be best at the lowest concentrations studied. Unfortunately activity coefficients predicted by equation (5.4.11) are reliable only for solutions with ionic strengths below about 0.1 mol dm^{-3}. Better predictions could be obtained if accurate activity data were available for the entire concentration range studied. We could then include the

FIGURE 5.4.1: Measured and Predicted Ternary Diffusion Coefficients for $CuSO_4(1) + H_2SO_4(2) + H_2O$ at 25°C: Δ, $C_1 + C_2 = 0.01$ mol dm^{-3}; 0, $C_1 + C_2 = 0.1$ mol dm^{-3}; □, $C_1 + C_2 = 0.5$ mol dm^{-3}.

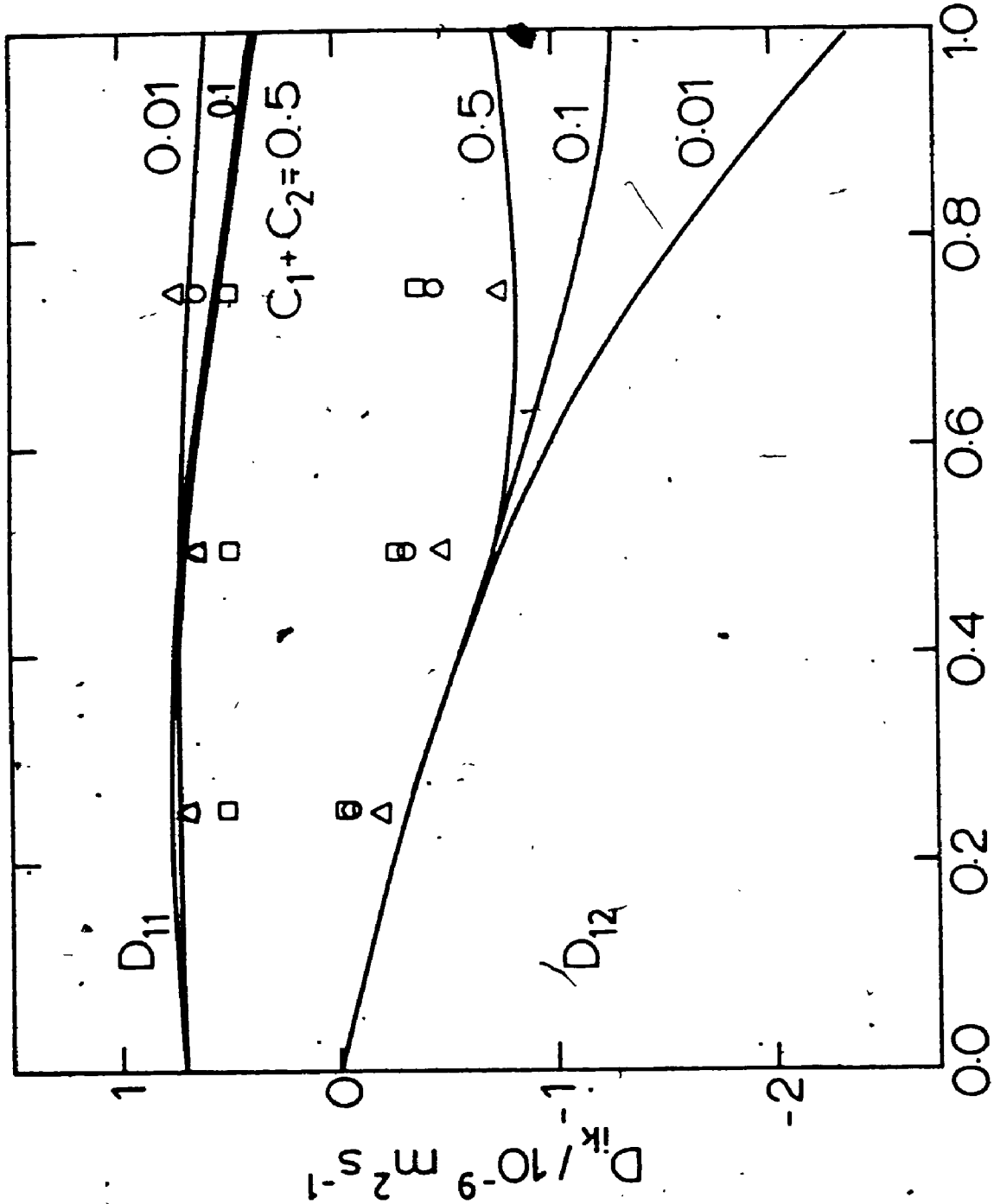
$D_{ik}/10^{-9}\ m^2 s^{-1}$
1
0
-1
-2
0.0
0.2
0.4
0.6
0.8
1.0
$C_1/(C_1+C_2)$
$C_1+C_2=0.5$
0.01
0.1
0.5
0.1
0.01
D_{11}
D_{12}

FIGURE 5.4.2: Measured and Predicted Ternary Diffusion Coefficients for $CuSO_4(1) + H_2SO_4(2) + H_2O$ at 25°C: Δ, $C_1 + C_2 = 0.01$ mol dm^{-3}; 0, $C_1 + C_2 = 0.1$ mol dm^{-3}; □, $C_1 + C_2 = 0.5$ mol dm^{-3}.

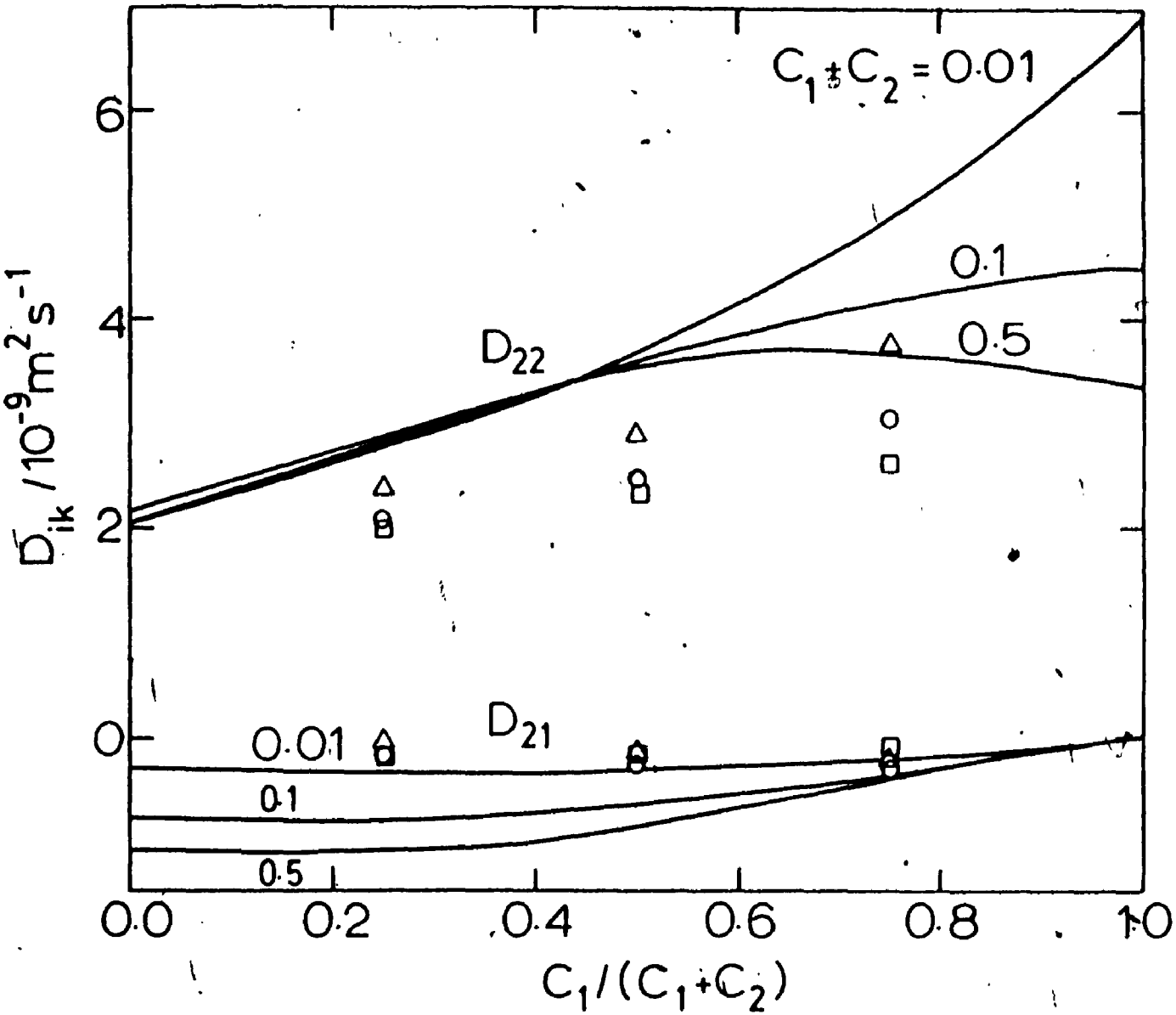
$C_1+C_2=0.01$
0.1
0.5
D_{22}
D_{21}
0.01
0.1
0.5
$D_{ik}/10^{-9}m^2s^{-1}$
$C_1/(C_1+C_2)$
0.0
0.2
0.4
0.6
0.8
1.0
0
2
4
6

multicomponent electrophoretic corrections[3,64,65] to make better theoretical predictions. But because these corrections are small (usually only a few percent of the the ℓ_{ik} coefficients), the electrophoretic terms are included only if accurate activity data are available.

A relationship between the apparent diffusivity (D^a_{11}) and the true diffusivity (D_{11}) of the copper sulfate component can be obtained by combining equations (5.1.1) and (5.1.2).

$$D^a_{11} = D_{11}[1+(D_{12}/D_{11})(\nabla C_2/\nabla C_1)] \qquad (5.4.21)$$

Because D^a_{11} measures the flux of $CuSO_4$ driven by the gradients in $CuSO_4$ and H_2SO_4, and D_{11} measures the flux of $CuSO_4$ driven by the $CuSO_4$ gradient alone, for solutions that have non-zero H_2SO_4 gradients, D^a_{11} and D_{11} will take different values.

Consider a diaphragm cell experiment[1,2a] with an initial $CuSO_4$ gradient (upper solution more dilute) with identical concentrations of H_2SO_4 in the upper and lower compartments. The upwards flow of $CuSO_4$ will produce substantial counterflow of H_2SO_4 into the lower compartment. Hence for $t > 0$, a non-zero H_2SO_4 gradient will exist as a result of coupled diffusion. In addition to the main flow of $CuSO_4$ driven by the salt's gradient ($-D_{11}\nabla C_1$), the H_2SO_4 gradient will cause counterflow of $CuSO_4$ ($-D_{12}\nabla C_2$). Hence D^a_{11} will be less than D_{11}.

Using the experimental diffusion coefficients listed in Table 5.4.1, equation (5.2.12) and integrated Fick equations[83]

$$\Delta C_i = [((D_{ii}-D_2)\Delta C_i^\circ + D_{ij}\Delta C_j^\circ)/(D_1-D_2)]e^{-\beta D_1 t} + [((D_{ii}-D_1)\Delta C_i^\circ + D_{ij}\Delta C_j^\circ)/(D_2-D_1)]e^{-\beta D_2 t} \quad (5.4.22)$$

$$(i,j = 1,2;\ i \neq j)$$

$$D_i = \tfrac{1}{2}[D_{11}+D_{22} + (-1)^{i+1}((D_{11}-D_{22})^2 + 4D_{12}D_{21})^{1/2}] \quad (5.4.23)$$

$$(i = 1,2)$$

where ΔC_i° and ΔC_j° are the initial concentration gradients across the diaphragm for solutes i and j respectively, numerical simulation of the diaphragm cell experiment described above indicates that the values of D_{11}^a are 1 to 8% smaller than D_{11}. Except for very short times or very long times, the coupled flow of H_2SO_4 into the lower solution compartment ($-D_{21}\nabla C_1$) is nearly balanced by the backflow of H_2SO_4 down its own gradient ($-D_{22}\nabla C_2$). Hence $J_2 = 0$ and from equation (5.1.3).

$$\nabla C_2/\nabla C_1 = -D_{21}/D_{22} \quad (5.4.24)$$

Substitution of equation (5.4.24) into equation (5.4.21) yields

$$D_{11}^a = D_{11}[1-(D_{12}D_{21}/D_{11}D_{22})] \quad (5.4.25)$$

a direct relationship between the apparent and multicomponent diffusivities.

5.5 Summary and Conclusions

Diffusion coefficients of $CuSO_4 + H_2SO_4 + H_2O$ mixtures have been determined at 25°C using conductimetric and diaphragm cell techniques. Measurements indicate that diffusion of sulfuric acid can produce large coupled flows of copper sulfate and vice versa. If diffusion of copper sulfate is treated as a binary process, the measured pseudo-binary diffusivities are 1 to 8% lower than the salt's true diffusivity.

CHAPTER SIX

DIFFUSION IN A FOUR COMPONENT SYSTEM: POTASSIUM CHLORIDE + POTASSIUM DIHYDROGEN PHOSPHATE + PHOSPHORIC ACID + WATER MIXTURES

6.1 Introduction

Diffusion data for four-component systems are sparse. Prior to this work, quaternary diffusion data had been reported only for the non-electrolyte acetone + chloroform + methanol + benzene system.[73] Recently, diffusion coefficients were measured for the quaternary electrolyte system HCl + NaCl + NaI + H_2O.[84] This work explores quaternary diffusion in the system KCl + KH_2PO_4 + H_3PO_4 + H_2O.

Measurements for this system can provide information about coupled flow of $\widehat{KCl}$ driven by pH gradients in KH_2PO_4 + H_3PO_4 + H_2O buffers and provide insight into proton-coupled transport of salts. Additionally, diffusion data for H_3PO_4 in KCl solutions can provide information about diffusion of a weak electrolyte in a supporting salt solution.

KCl + KH_2PO_4 + H_3PO_4 + H_2O is one of the few quaternary systems for which precise activity data is available.[85,86] Hence, the experimental diffusion coefficients for this system can be used to evaluate Onsager transport coefficients and to test the Onsager

reciprocal relations[66,67] for isothermal quaternary diffusion. Along with reported species mobilities,[2e,87] the calculated activity coefficients and the binary diffusivities of the three components,[88-91] a complete analysis of the diffusional properties can be made. Additionally, all three components can be obtained with high purity, eliminating the need for further purification.

It will also be shown that transformation of transport coefficients for this system will allow coefficients for the system KCl + KH_2PO_4 + HCl + H_2O to be obtained. It should be noted that the choice KCl + KH_2PO_4 + HCl + H_2O is arbitrary; coefficients for other systems such as KCl + HCl + H_3PO_4 + H_2O and HCl + KH_2PO_4 + H_3PO_4 + H_2O could have as easily been obtained.

6.2 Experimental Procedure

Quaternary diffusion coefficients were determined by the magnetically stirred diaphragm cell method[1,2a] of Stokes. Details of the cell and procedure are given in Sections 5.2 and 5.3.

Determination of the diffusion coefficients requires three independent diaphragm cell runs A, B and C to be carried out with different initial concentration differences ($\Delta C^A(0)$, $\Delta C^B(0)$ and $\Delta C^C(0)$) across the diaphragm. X is given by[51,73]

$$\mathbf{X} = \begin{bmatrix} \Delta C_1^A(0) & \Delta C_1^B(0) & \Delta C_1^C(0) \\ \Delta C_2^A(0) & \Delta C_2^B(0) & \Delta C_2^C(0) \\ \Delta C_3^A(0) & \Delta C_3^B(0) & \Delta C_3^C(0) \end{bmatrix} \begin{bmatrix} \Delta C_1^A(t_f) & \Delta C_1^B(t_f) & \Delta C_1^C(t_f) \\ \Delta C_2^A(t_f) & \Delta C_2^B(t_f) & \Delta C_2^C(t_f) \\ \Delta C_3^A(t_f) & \Delta C_3^B(t_f) & \Delta C_3^C(t_f) \end{bmatrix}^{-1} \quad (6.2.1)$$

Equation (5.2.15) then yields the integral diffusion coefficients.

Stock solutions made up from twice-distilled, deionized water and reagent grade KCl, KH_2PO_4 and H_3PO_4 were filtered and used without further purification. Concentrations of $KCl(C_1)$, $KH_2PO_4(C_2)$ and $H_3PO_4(C_3)$ were determined by titration of duplicate 0.010 dm^{-3} samples of solution. Titration with silver nitrate gave C_1. Excess chloride was added to precipitate any free silver ion; then titration with standardized sodium hydroxide to endpoints near pH 5 and 9 gave C_2 and C_3.[74b] C_1, C_2 and C_3 values were reproducible to 0.10, 0.25 and 0.20% respectively.

6.3 Results and Discussion

Quaternary diffusion coefficients for aqueous $KCl(C_1)$ + $KH_2PO_4(C_2)$ + $H_3PO_4(C_3)$ mixtures were determined at a total electrolyte concentration of 0.06 mol dm^{-3} for $C_1:C_2:C_3$ ratios of 2:1:3, 2:2:2 and 2:3:1. The results listed in Table 6.3.1 are averaged values from three separate experiments for each concentration ratio. Precision of the data is listed as ± two standard

TABLE 6.3.1

Quaternary Diffusion Coefficients[a,b] for KCl(1) + KH_2PO_4(2) + H_3PO_4(3) + H_2O at 25°C

	C_1 = 0.020 C_2 = 0.010 C_3 = 0.030	C_1 = 0.020 C_2 = 0.020 C_3 = 0.020	C_1 = 0.020 C_2 = 0.030 C_3 = 0.010
D_{11}	1.94 ± 0.05 (1.95)	1.92 ± 0.05 (1.95)	1.94 ± 0.05 (1.95)
D_{12}	-0.14 ± 0.05 (-0.26)	-0.03 ± 0.01 (-0.08)	0.075 ± 0.006 (0.07)
D_{13}	0.40 ± 0.03 (0.41)	0.43 ± 0.03 (0.44)	0.48 ± 0.05 (0.42)
D_{21}	-0.05 ± 0.05 (-0.08)	-0.08 ± 0.24 (-0.10)	-0.06 ± 0.03 (-0.10)
D_{22}	2.21 ± 0.11 (2.39)	1.78 ± 0.05 (1.93)	1.44 ± 0.07 (1.41)
D_{23}	-1.04 ± 0.02 (-1.07)	-1.19 ± 0.09 (-1.35)	-1.60 ± 0.22 (-1.51)
D_{31}	0.03 ± 0.02 (0.04)	0.02 ± 0.02 (0.04)	0.07 ± 0.01 (0.03)
D_{32}	-1.36 ± 0.07 (-1.67)	-0.93 ± 0.05 (-1.14)	-0.53 ± 0.04 (-0.53)
D_{33}	2.02 ± 0.07 (2.10)	2.27 ± 0.06 (2.44)	2.84 ± 0.16 (2.64)

[a] Predicted values in parentheses

[b] Units: C_i in mol dm^{-3}; D_{ik} in 10^{-9} m^2 s^{-1}

deviations. The major sources of errors are the determination of the cell constant and concentration differences.

The measured diffusion coefficients listed in Table 6.3.1 are not differential coefficients but rather integral values which represent averages of differential coefficients over the range of composition from the mean composition of the upper compartment ($\bar{C}_{1U}$, $\bar{C}_{2U}$, $\bar{C}_{3U}$) to the mean composition of the lower compartment ($\bar{C}_{1L}$, $\bar{C}_{2L}$, $\bar{C}_{3L}$).[2a] (See Section 3.4 for a similar discussion on binary diffusion.) Numerical integration of predicted diffusion coefficients

$$\bar{D}_{ik} = \int_0^1 D_{ik}(C_1, C_2, C_3)d\epsilon \qquad (6.3.1)$$

with

$$\epsilon = (C_i - \bar{C}_{iU})/(\bar{C}_{iL} - \bar{C}_{iU}) \qquad (6.3.2)$$

indicated that differences between the integral and differential values calculated at the mean cell composition ($\epsilon = 0.5$) could be neglected as they were well within our experimental error.

The system KCl + KH_2PO_4 + H_3PO_4 + H_2O contains five major solute species (Cl^-, K^+, $H_2PO_4^-$, H^+ and undissociated H_3PO_4 molecules). Because of electroneutrality and local

chemical equilibrium, only three solute flows are independent. Hence the diffusional properties of the system are quaternary.

The solute species, constituent ions and components are numbered as follows:

Species	Ions	Components
1. Cl^-	1. Cl^-	1. KCl
2. K^+	2. K^+	2. KH_2PO_4
3. $H_2PO_4^-$	3. $H_2PO_4^-$	3. H_3PO_4
4. H^+	4. H^+	
5. H_3PO_4		

which define the stoichiometric coefficients as

$$\nu = \begin{pmatrix} 1 & 0 & 0 \\ 1 & 1 & 0 \\ 0 & 1 & 1 \\ 0 & 0 & 1 \end{pmatrix} \qquad (6.3.3)$$

and

$$\nu = \begin{pmatrix} 1 & 0 & 0 & 0 & 0 \\ 0 & 1 & 0 & 0 & 0 \\ 0 & 0 & 1 & 0 & 1 \\ 0 & 0 & 0 & 1 & 1 \end{pmatrix} \qquad (6.3.4)$$

Estimates of the Onsager coefficients for the species

$$\mathbf{\Lambda} = \begin{pmatrix} \Lambda_{11} & 0 & 0 & 0 & 0 \\ 0 & \Lambda_{22} & 0 & 0 & 0 \\ 0 & 0 & \Lambda_{33} & 0 & 0 \\ 0 & 0 & 0 & \Lambda_{44} & 0 \\ 0 & 0 & 0 & 0 & \Lambda_{55} \end{pmatrix} \quad (6.3.5)$$

and equations (2.5.7), (6.3.4) and (6.3.5) yield

$$\mathbf{\Lambda} = \begin{pmatrix} \Lambda_{11} & 0 & 0 & 0 \\ 0 & \Lambda_{22} & 0 & 0 \\ 0 & 0 & \Lambda_{33} + \Lambda_{55} & \Lambda_{55} \\ 0 & 0 & \Lambda_{55} & \Lambda_{44} + \Lambda_{55} \end{pmatrix} \quad (6.3.6)$$

The Λ_{iK} are given by equations (2.5.13) and (3.4.2) and published limiting molar conductances.[2e,87] Calculations give $D_1(Cl^-) = 2.033 \times 10^{-9}$, $D_2(K^+) = 1.957 \times 10^{-9}$, $D_3(H_2PO_4^-) = 0.860 \times 10^{-9}$ and $D_4(H^+) = 9.315 \times 10^{-9}$ $m^2\ s^{-1}$ for the ionic diffusivities. For the diffusivity of molecular H_3PO_4, we will use the value $D_5(H_3PO_4) = 0.870 \times 10^{-9}$ $m^2\ s^{-1}$ obtained by analysis of binary diffusion data for $H_3PO_4 + H_2O$ solutions.[90]

Species concentrations can be calculated from

$$c_1(Cl^-) = C_1 \qquad (6.3.7)$$

$$c_2(K^+) = C_1 + C_2 \qquad (6.3.8)$$

$$c_3(H_2PO_4^-) = B'C_3 + C_2 \qquad (6.3.9)$$

$$c_4(H^+) = B'C_3 \qquad (6.3.10)$$

$$c_5(H_3PO_4) = (1-B')C_3 \qquad (6.3.11)$$

where B' is the degree of dissociation of H_3PO_4

$$B' = [H^+]/C_3 \qquad (6.3.12)$$

Values of B' are obtained from the equilibrium condition

$$K = [B'(C_2+B'C_3)y_3y_4]/[(1-B')y_0] \qquad (6.3.13)$$

At 25°C, K = 7.14 x 10^{-3} mol dm^{-3}.[86] y_0 is the activity coefficient for the undissociated H_3PO_4 molecule.

Evaluation of equation (6.3.13) requires accurate activity data for the quaternary mixtures. Fortunately, precise molar activity coefficients, γ_i can be calculated from Pitzer and Sylvester's semiempirical expressions for the KCl(1) + KH_2PO_4(2) + H_3PO_4(3) + H_2O system. In simplest form[85,86]

$$\ln\gamma_{KCl} = f' + m_{Cl^-}(B_{KCl} + m_{H_2PO_4^-}(B_{KH_2PO_4} + \theta_{Cl^-,H_2PO_4^-}) + m_{K^+}B_{KCl} + m_{H^+}(B_{HCl} + \theta_{H^+,K^+}) + m_{H_3PO_4}\lambda_{K^+,H_3PO_4} \quad (6.3.14)$$

$$\ln\gamma_{KH_2PO_4} = f' + m_{Cl^-}(B_{KCl} + \theta_{H_2PO_4^-,Cl^-}) + m_{H_2PO_4^-}B_{KH_2PO_4} + m_{K^+}B_{KH_2PO_4} + m_{H^+}\theta_{H^+,K^+} + m_{H_3PO_4}(\lambda_{K^+,H_3PO_4} + \lambda_{H_2PO_4^-,H_3PO_4}) \quad (6.3.15)$$

$$\ln\gamma_{H_3PO_4} = f' + m_{Cl^-}(B_{HCl} + \theta_{H_2PO_4^-,Cl^-}) + m_{K^+}(B_{KH_2PO_4} + \theta_{H^+,K^+}) + m_{H_3PO_4}(\lambda_{H^+,H_3PO_4} + \lambda_{H_2PO_4^-,H_3PO_4}) \quad (6.3.16)$$

$$f' = -0.392\,[(I^{1/2}/(1 + 1.2\,I^{1/2})) + ((2/1.2)\ln(1 + 1.2\,I^{1/2}))] \quad (6.3.17)$$

Values of the parameters needed to evaluate equations (6.3.14)-(6.3.16) are listed in Table 6.3.2. Check calculations indicated that the small differences between γ_i and y_i could be neglected without causing significant error.[28] I, the ionic strength, can be expressed as

$$I = C_1 + C_2 + B'C_3 \quad (6.3.18)$$

Following the procedure in Sections 4.4 and 5.4 the Onsager coefficients for the three solute components can be found.

TABLE 6.3.2

Supplemental Data[a,c] for Calculation of Activity Coefficients from Pitzer's Equations for KCl(1) + KH_2PO_4(2) + H_3PO_4(3) + H_2O at 25°C

$C_1:C_2:C_3$[b]	B_{KCl}[b]	$B_{KH_2PO_4}$[b]	B_{HCl}[b]
20.0/10.0/30.0	0.211	-0.148	0.404
20.0/20.0/20.0	0.209	-0.147	0.400
20.0/30.0/10.0	0.206	-0.145	0.396

a $\theta_{Cl^-,H_2PO_4^-} = 0.10$ kg mol^{-1},

$\theta_{H^+,K^+} = 0.005$ kg mol^{-1},

$\lambda_{K^+,H_3PO_4} = -0.070$ kg mol^{-1},

$\lambda_{H_2PO_4^-,H_3PO_4} = -0.04$ kg mol^{-1},

$\lambda_{H^+,H_3PO_4} = 0.290$ kg mol^{-1}

b Units: C_i in 10^{-3} mol dm^{-3}; B_{KCl}, $B_{KH_2PO_4}$ and B_{HCl} in kg mol^{-1}

c Ref. 85, 86

$$L_{11} = (ce-d^2)/[a(ce-d^2)-b^2e] \quad (6.3.19)$$

$$L_{12} = L_{21} = -be/[a(ce-d^2)-b^2e] \quad (6.3.20)$$

$$L_{13} = L_{31} = bd/[a(ce-d^2)-b^2e] \quad (6.3.21)$$

$$L_{22} = ae/[a(ce-d^2)-b^2e] \quad (6.3.22)$$

$$L_{23} = L_{32} = -ad/[a(ce-d^2)-b^2e] \quad (6.3.23)$$

$$L_{33} = (ac-b^2)/[a(ce-d^2)-b^2e] \quad (6.3.24)$$

where

$$a = (\dot{\ell}_{11} + \dot{\ell}_{22})/\dot{\ell}_{11}\dot{\ell}_{22} \quad (6.3.25)$$

$$b = 1/\dot{\ell}_{22} \quad (6.3.26)$$

$$c = 1/\dot{\ell}_{22} + [(\dot{\ell}_{44} + \dot{\ell}_{55})/(\dot{\ell}_{33}\dot{\ell}_{44} + \dot{\ell}_{33}\dot{\ell}_{55} + \dot{\ell}_{44}\dot{\ell}_{55})] \quad (6.3.27)$$

$$d = \dot{\ell}_{44}/(\dot{\ell}_{33}\dot{\ell}_{44} + \dot{\ell}_{33}\dot{\ell}_{55} + \dot{\ell}_{44}\dot{\ell}_{55}) \quad (6.3.28)$$

$$e = (\dot{\ell}_{33} + \dot{\ell}_{44})/(\dot{\ell}_{33}\dot{\ell}_{44} + \dot{\ell}_{33}\dot{\ell}_{55} + \dot{\ell}_{44}\dot{\ell}_{55}) \quad (6.3.29)$$

Predicted L_{ik} coefficients are listed in Table 6.3.3.

The expressions for the chemical potentials of the components may be written as

$$\mu_1 = \mu_1^\circ + RT\ln[(C_1 + C_2)C_1 y_1^2] \qquad (6.3.30)$$

$$\mu_2 = \mu_2^\circ + RT\ln[(C_1 + C_2)(C_2 + B'C_3)y_2^2] \qquad (6.3.31)$$

$$\mu_3 = \mu_3^\circ + RT\ln[B'C_3(C_2 + B'C_3)y_3^2] \qquad (6.3.32)$$

Differentiation of Pitzer and Sylvester's equations, along with equations (6.3.12)-(6.3.13), (6.3.18) and (6.3.30)-(6.3.32) give the $\partial\mu_m/\partial C_k$ values listed in Table 6.3.4. The predicted diffusion coefficients listed in Table 6.3.1 are then obtained by the use of equation (2.4.3) and the values in Tables 6.3.3 and 6.3.4. Agreement between the experimental and predicted diffusion coefficients is good, within experimental error in most cases.

Experimental L_{ik} coefficients listed in Table 6.3.3 were calculated from the measured D_{ik} values and predicted $\partial\mu_m/\partial C_k$ values using equation (4.4.18). The precision of the data is quoted as ± two standard deviations. Because calculation of the L_{ik} coefficients requires taking differences between measured D_{ik} values, the relative precision of the measured L_{ik} is lower. Even so, $L_{12} = L_{21}$, $L_{23} = L_{32}$ and $L_{13} = L_{31}$, within the limits of our experimental error. Hence the Onsager reciprocal relationship[66,67] is satisfied. The agreement between the experimental and calculated L_{ik} coefficients is close, within experimental error in most cases.

TABLE 6.3.3

L_{ik} Coefficients[a,b] for KCl(1) + KH_2PO_4(2) + H_3PO_4(3) + H_2O at 25°C

	$C_1 = 0.020$ $C_2 = 0.010$ $C_3 = 0.030$	$C_1 = 0.020$ $C_2 = 0.020$ $C_3 = 0.020$	$C_1 = 0.020$ $C_2 = 0.030$ $C_3 = 0.010$
RTL_{11}	3.18 ± 0.23 (3.29)	3.14 ± 0.17 (3.22)	3.17 ± 0.17 (3.22)
RTL_{12}	-1.92 ± 0.29 (-2.16)	-1.46 ± 0.13 (-1.59)	-1.08 ± 0.10 (-1.10)
RTL_{13}	1.72 ± 0.23 (1.83)	1.09 ± 0.07 (1.13)	0.56 ± 0.11 (0.50)
RTL_{21}	-1.96 ± 0.34 (-2.16)	-1.45 ± 0.87 (-1.59)	-1.06 ± 0.22 (-1.10)
RTL_{22}	4.89 ± 0.54 (5.28)	4.27 ± 0.59 (4.66)	3.80 ± 0.46 (3.74)
RTL_{23}	-4.26 ± 0.29 (-4.46)	-2.93 ± 0.44 (-3.31)	-1.79 ± 0.45 (-1.70)
RTL_{31}	1.57 ± 0.61 (1.83)	0.93 ± 0.15 (1.13)	0.58 ± 0.10 (0.50)
RTL_{32}	-3.82 ± 0.39 (-4.46)	-2.78 ± 0.29 (-3.31)	-1.76 ± 0.27 (-1.70)
RTL_{33}	6.57 ± 0.50 (6.96)	4.75 ± 0.29 (5.16)	2.90 ± 0.33 (2.70)

[a] Predicted values in parentheses

[b] Units: C_i in mol dm^{-3}; L_{ik} in 10^{-10} mol m^{-1} s^{-1}

TABLE 6.3.4

Values of $\partial\mu_m/\partial C_k$[a,b,c] for KCl(1) + KH_2PO_4(2) + H_3PO_4(3) + H_2O at 25°C

	C_1 = 0.020 C_2 = 0.010 C_3 = 0.030 B' = 0.34	C_1 = 0.020 C_2 = 0.020 C_3 = 0.020 B' = 0.29	C_1 = 0.020 C_2 = 0.030 C_3 = 0.010 B' = 0.25
μ_{11}/RT	79.63	71.67	67.02
μ_{22}/RT	67.00	54.56	45.09
μ_{33}/RT	37.40	52.64	101.67
μ_{12}/RT	30.06	21.64	16.70
μ_{13}/RT	-1.08	-0.97	-0.84
μ_{23}/RT	11.07	8.10	5.68

[a] $\mu_{mk} = (\partial\mu_m/\partial C_k)_{T,p,C_{q\neq k}}$

[b] $\mu_{12}/RT = \mu_{21}/RT$; $\mu_{13}/RT = \mu_{31}/RT$; $\mu_{23}/RT = \mu_{32}/RT$

[c] Units: C_i in mol dm^{-3}; μ_{mk}/RT in dm^3 mol^{-1}

Figure 6.3.1 displays the measured and predicted diffusion coefficients for total solute concentration of 0.0600 mol dm^{-3} and KCl concentration of 0.0200 mol dm^{-3}. The coefficients are plotted against $C_2/(C_2 + C_3)$, the fraction of KH_2PO_4 in the $KH_2PO_4 + H_3PO_4 + H_2O$ buffer mixture.

Measured values of D_{33}, the quaternary diffusivity of the H_3PO_4 component, range from 2.02-2.84 x 10^{-9} m^2 s^{-1}. At similar concentrations, the binary diffusion coefficients of aqueous H_3PO_4 are considerably smaller,[89,90] about 1.0 x 10^{-9} m^2 s^{-1}. In binary solutions, however, H^+ ions are constrained by electroneutrality to diffuse at the same rate as the less mobile $H_2PO_4^-$ ions. The electric field that is set up by the diffusing H^+ ions tends to slow that ion down and speed up the less mobile ion. In mixed electrolyte solutions, H^+ ions can diffuse much more rapidly while still maintaining electroneutrality by generating concurrent flow of Cl^- ions and countercurrent flow of K^+ ions. Consequently, cross-coefficients D_{13} and D_{23} are positive and negative respectively.

D_{22}, the quaternary diffusivity of the KH_2PO_4 component (1.44-2.21 x 10^{-9} m^2 s^{-1}), is also larger than its binary diffusivity[91] (approximately 1.4 x 10^{-9} m^2 s^{-1}). When KH_2PO_4 diffuses in pure water, the diffusion induced electric field slows down K^+ ions and speeds up $H_2PO_4^-$ ions. In the quaternary mixtures under

FIGURE 6.3.1: Measured and Predicted Quaternary Diffusion Coefficients for KCl [0.02 mol·dm^{-3}] + KH_2PO_4 [(x) 0.04 mol dm^{-3}] + H_3PO_4 [(1-x) 0.04 mol dm^{-3}] + H_2O at 25°C where $x = C_2(KH_2PO_4)/[C_2(KH_2PO_4) + C_3(H_3PO_4)]$.

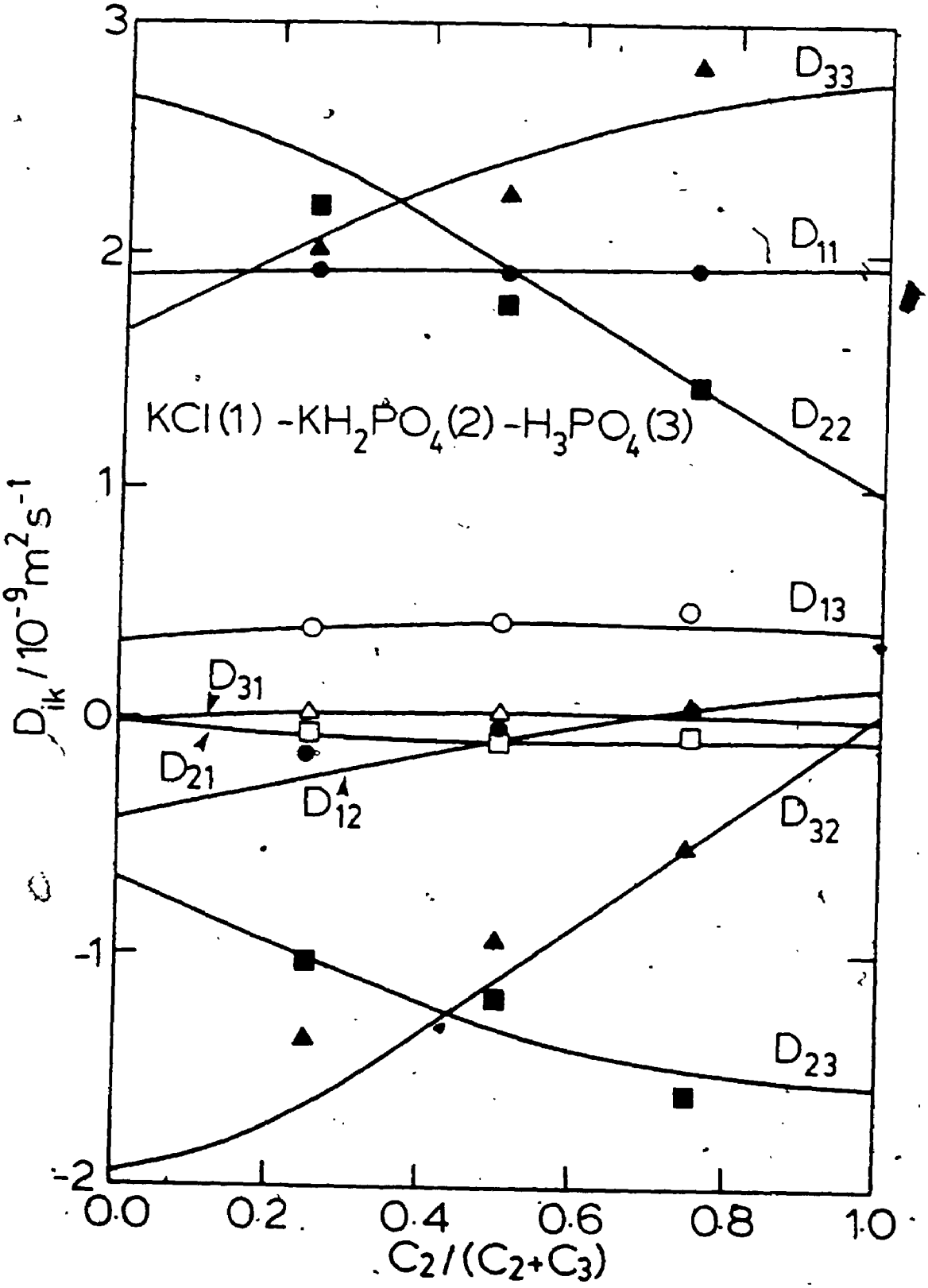
KCl(1) -KH2PO4(2) -H3PO4(3)
D33
D11
D22
D13
D31
D21
D12
D32
D23
Dik / 10-9 m2 s-1
C2/(C2+C3)
3
2
1
0
-1
-2
0.0
0.2
0.4
0.6
0.8
1.0

consideration, the electric field should drive concurrent flow of Cl^- and counterflow of H^+ ions. Consequently, values for D_{12} and D_{32} should be positive and negative respectively. From Table 6.3.1, it is clear that values of D_{32} are negative. However, D_{12} values are positive for KH_2PO_4-rich mixtures but become negative for H_3PO_4-rich mixtures. This means that coupled flow of KCl driven by KH_2PO_4 gradients can change direction.

A gradient in concentration of KH_2PO_4 in a H_3PO_4-rich mixture will produce an opposite gradient of similar magnitude in the concentration of H^+ ions. As the H^+ ions diffuse down their gradient toward the KH_2PO_4-rich region of the solution, an electric field is generated to slow them down in order to maintain electroneutrality. Since the electric field will drive Cl^- ion towards the KH_2PO_4 region, values of D_{12} are negative.

D_{11}, the quaternary diffusivity of the KCl component, is equal to the salt's binary diffusivity[88] within experimental error. Because the difference in mobilities between K^+ and Cl^- ions is small, relatively weak electric fields are generated. Consequently, values of D_{21} and D_{31} are small.

By examining the left-hand intercepts of Figure 6.3.1, information about diffusion of a weak electrolyte (H_3PO_4) in a salt solution (KCl) can be obtained. This might seem to be an example of ternary diffusion. However, in KCl + H_3PO_4 + H_2O mixtures, there are five major solute

species (K^+, Cl^-, H^+, $H_2PO_4^-$ and undissociated H_3PO_4) with only two constraints (electroneutrality and local equilibrium of dissociation of H_3PO_4 molecules). Therefore three independent flows exist and the diffusion properties are quaternary. Without added KH_2PO_4, it would appear that D_{21} and D_{23} should equal zero. Examination of Figure 6.3.1 indicates that values of D_{23} are large and negative, even though there is no added KH_2PO_4 for the H_3PO_4 component to drive. When KCl and H_3PO_4 components interdiffuse, H^+ ions will migrate rapidly into the KCl solution. Because slower $H_2PO_4^-$ ions are left behind, the KH_2PO_4 concentration builds up in the H_3PO_4-rich portion of the solution.

Finally, we consider how predictions for other related systems such as KCl + KH_2PO_4 + HCl + H_2O can be obtained. The concentrations of KCl(C_1) + KH_2PO_4(C_2) + H_3PO_4(C_3) + H_2O solutions are related to concentations of KCl (C_1') + KH_2PO_4(C_2') + HCl(C_3') + H_2O solutions by

$$C_i' = \sum_{k=1}^{3} A_{ik} C_k \qquad (6.3.33)$$

where $A_{11} = A_{22} = A_{33} = A_{23} = 1$, $A_{12} = A_{21} = A_{31} = A_{32} = 0$ and $A_{13} = -1$. By using the linear transformation[92]

$$\bar{D}' = A\,D\,A^{-1} \qquad (6.3.34)$$

diffusion coefficients D'_{ik} of the KCl + KH_2PO_4 + HCl + H_2O system can be obtained from coefficients of the KCl + KH_2PO_4 + H_3PO_4 + H_2O system.

$$D'_{11} = D_{11} - D_{31} \qquad (6.3.35)$$

$$D'_{12} = D_{12} - D_{32} \qquad (6.3.36)$$

$$D'_{13} = D_{11}-D_{12} + D_{13}-D_{31} + D_{32}-D_{33} \qquad (6.3.37)$$

$$D'_{21} = D_{21} + D_{31} \qquad (6.3.38)$$

$$D'_{22} = D_{22} + D_{32} \qquad (6.3.39)$$

$$D'_{23} = D_{21}-D_{22} + D_{23}+D_{31} - D_{32}+D_{33} \qquad (6.3.40)$$

$$D'_{31} = D_{31} \qquad (6.3.41)$$

$$D'_{32} = D_{32} \qquad (6.3.42)$$

$$D'_{33} = D_{31}-D_{32} + D_{33} \qquad (6.3.43)$$

Table 6.3.5 gives experimental diffusion coefficients D'_{ik} for aqueous KCl + KH_2PO_4 + HCl mixtures that were calculated from the data listed in Table 6.3.1.

Values of D'_{11} are very close to the D_{11} values determined for the KCl + KH_2PO_4 + H_3PO_4 + H_2O system. D'_{21}

TABLE 6.3.5

Quaternary Diffusion Coefficients[a] for $KCl(1') + KH_2PO_4(2') + HCl(3') + H_2O$ at 25°C

	$C_1' = -0.010$ $C_2' = 0.040$ $C_3' = 0.030$	$C_1' = 0.000$ $C_2' = 0.040$ $C_3' = 0.020$	$C_1' = 0.010$ $C_2' = 0.040$ $C_3' = 0.010$
D_{11}'	1.91	1.90	1.87
D_{12}'	1.22	0.90	0.61
D_{13}'	-0.93	-0.84	-1.10
D_{21}'	-0.02	-0.06	0.01
D_{22}'	0.85	0.85	0.91
D_{23}'	0.11	0.17	0.34
D_{31}'	0.03	0.02	0.07
D_{32}'	-1.36	-0.93	-0.53
D_{33}'	3.41	3.22	3.44

[a] Units: C_i' in mol dm^{-3}; D_{ik}' in 10^{-9} m^2 s^{-1}

and D'_{31} are again both small indicating that the KCl component does not generate a very significant flux of either of the other two components. D'_{33}, the quaternary diffusivity of the HCl component, ranges from $3.22\text{-}3.44 \times 10^{-9}$ m^2 s^{-1}. At similar concentrations, the binary diffusion coefficient of aqueous HCl is approximately 3.14×10^{-9} m^2 s^{-1}, about 10% lower.[93]

The calculated value for D'_{22}, the quaternary diffusivity of the KH_2PO_4 component, is approximately 0.87×10^{-9} m^2 s^{-1}, nearly 20% lower than the binary diffusivity of KH_2PO_4 in water.[91] In contrast, D_{22} for KCl + KH_2PO_4 + H_3PO_4 + H_2O mixtures is much larger than the salt's binary diffusivity. When a gradient in concentration of KH_2PO_4 is formed in a uniform solution of HCl, H^+ will diffuse to the KH_2PO_4-rich region to replenish free H^+ lost by the association reaction $H^+ + H_2PO_4^- \rightleftharpoons H_3PO_4$. The generated electric field will slow down countercurrent migration of $H_2PO_4^-$, thus reducing the diffusivity of the KH_2PO_4 component.

The diaphragm cell technique of Stokes is well suited to the determination of quaternary diffusion coefficients. The task involves the relatively easy measurement of the concentration of each solute component. Free diffusion experiments[94,95] have shown that coupled flows of electrolytes can produce density inversions and consequently, mixing within the cell. However with diaphragm cell experiments, errors due to convectional

mixing are eliminated by confining diffusion to the pores of the diaphragm.

6.4 Summary and Conclusions

Stokes diaphragm cells were used to measure quaternary diffusion coefficients for three compositions of the system KCl + KH_2PO_4 + H_3PO_4 + H_2O at 25°C. Measurements show that pH gradients produced by KH_2PO_4 + H_3PO_4 + H_2O buffers can drive large coupled flows of KCl which can concentrate KCl within the diffusion boundaries. Quaternary diffusivities of the KH_2PO_4 and H_3PO_4 components are much larger than the binary diffusivities of the aqueous components. It was demonstrated that Onsager's reciprocal relations $L_{12} = L_{21}$, $L_{23} = L_{32}$ and $L_{13} = L_{31}$ for isothermal quaternary diffusion hold. By transformation of transport coefficients for the system KCl + KH_2PO_4 + H_3PO_4 + H_2O, coefficients for the system KCl + KH_2PO_4 + HCl + H_2O are obtained.

APPENDIX ONE

Sample Data[a] for the Computation of the Binary Diffusion Coefficients for NaOH + H_2O at 25°C

t[b]	R_T[b]	R_B[b]	$\ln\Delta K$
33025	43640.000	2499.199	-7.9306
56121	20966.000	2850.067	-8.1536
61340	18720.000	2925.263	-8.2047
67350	16716.000	3009.225	-8.2632
118290	9400.000	3622.803	-8.7563
124339	9034.100	3687.097	-8.8145
141683	8206.600	3863.562	-8.9827
147011	8004.000	3914.884	-9.0344
206464	6612.000	4379.853	-9.6107
212739	6528.700	4420.450	-9.6712
219874	6442.618	4464.852	-9.7401
231090	6323.600	4530.953	-9.8484

Average D = 2.0432 x 10^{-9} m^2 s^{-1}, Standard deviation in D = 0.0024 x 10^{-9} m^2 s^{-1}

[a] C_∞ = 0.00662 mol dm^{-3}; a = 0.04563 m; r = 0.9559

[b] Units: t in s; R_T and R_B in ohms

APPENDIX TWO

Sample Data[a] File for the Harned Experiment with the Gradient in NaOH for NaOH + NaCl + H_2O at 25°C

t[b]	R_T[b]	R_B[b]
77399	4441.659	1204.008
83105	4187.000	1234.220
92395	3841.598	1281.799
99337	3629.500	1315.505
106945	3432.532	1350.857
117918	3203.000	1399.825
162645	2635.434	1563.068
173768	2549.205	1596.405
181997	2494.900	1619.463
186369	2468.501	1631.157
191970	2438.089	1645.839
208172	2360.862	1684.771
250097	2222.900	1764.690
257878	2203.013	1775.644
262943	2191.327	1782.684
269422	2179.450	1792.386
274134	2171.113	1799.067
278923	2162.933	1805.609
336199	2087.958	1863.478
342048	2081.767	1867.343
349162	2075.391	1872.335
359290	2067.302	1879.020
366193	2062.633	1883.447
376147	2057.681	1890.330

Sample Data[a] File for the Harned Experiment with the Gradient in NaCl for NaOH + NaCl + H_2O at 25°C

t[b]	R_T[b]	R_B[b]
79457	2217.484	1689.563
84422	2212.686	1696.730
90558	2207.000	1705.569
95096	2203.653	1712.600
99441	2199.300	1718.600
104311	2194.424	1725.075
174365	2119.840	1794.571
178448	2115.320	1797.257
184497	2111.400	1802.911
189634	2107.500	1806.971
194712	2103.500	1810.816
200291	2099.000	1814.838
251380	2063.774	1844.408
256566	2060.415	1846.741
270648	2051.427	1852.078
274724	2049.633	1854.003
285200	2045.100	1858.640
291466	2042.600	1861.252
336862	2025.668	1876.366
342262	2024.000	1877.690
347707	2020.866	1878.293
353770	2018.832	1879.239
363707	2018.486	1883.626
379225	2015.817	1888.667

[a] C_{NaOH} = 0.01506 mol dm^{-3}, C_{NaCl} = 0.00494 mol dm^{-3}; a = 0.04563 m; $r_{av.}$ = 0.9723

[b] Units: t in s; R_T and R_B in ohms

APPENDIX THREE

Sample Data[a] for the Computation of the Ternary Diffusion Coefficients for NaOH + NaCl + H_2O at 25°C

(X_1 = 0.6417)

t[b]	$\Delta K_1(t)/\Delta K_1(0)$	$\Delta K_2(t)/\Delta K_2(0)$	D_a[b]
77399	0.44299	0.73588	1.7117
83105	0.41769	0.71866	1.7111
92395	0.37935	0.70655	1.7098
99337	0.35316	0.69667	1.7089
106945	0.32659	0.68968	1.7079
117918	0.29178	0.68780	1.7063
162645	0.18616	0.39048	1.7029
173768	0.16665	0.39140	1.7017
181997	0.15365	0.37888	1.7012
186369	0.14716	0.36493	1.7010
191970	0.13932	0.35318	1.7008
208172	0.11888	0.35120	1.6993
250097	0.07926	0.23882	1.7119
257878	0.07363	0.23137	1.7109
262943	0.07016	0.20477	1.7119
269422	0.06605	0.19990	1.7109
274134	0.06320	0.18293	1.7115
278923	0.06040	0.17424	1.7113

Average D_a = 1.7073 x 10^{-9} m^2 s^{-1}, Standard Deviation in D_a = 0.0047 x 10^{-9} m^2 s^{-1}

(X_2 = 1.2064)

t[b]	$\Delta K_1(t)/\Delta K_1(0)$	$\Delta K_2(t)/\Delta K_2(0)$	D_a[b]
77399	0.44299	0.73588	2.5857
83105	0.41769	0.71866	2.5857
92395	0.37935	0.70655	2.5856
99337	0.35316	0.69667	2.5855
106945	0.32659	0.68968	2.5854
117918	0.29179	0.68780	2.5852
162645	0.18616	0.39048	2.5744
173768	0.16665	0.39140	2.5730
181997	0.15365	0.37888	2.5722
186369	0.14716	0.36493	2.5720
191970	0.13932	0.35318	2.5716
208172	0.11887	0.35121	2.5690
250097	0.07926	0.23882	2.5848
257878	0.07363	0.23137	2.5847
262943	0.07016	0.20477	2.5848
269422	0.06605	0.19990	2.5847
274134	0.06320	0.18293	2.5847
278923	0.06040	0.17424	2.5847

Average D_a = 2.5808 x 10^{-9} m^2 s^{-1}, Standard Deviation in D_a = 0.0064 x 10^{-9} m^2 s^{-1}

[a] C_{NaOH} = 0.01506 mol dm^{-3}, C_{NaCl} = 0.00494 mol dm^{-3}; S_1/S_2 = 2.2896

[b] Units: t in s; D_a in 10^{-9} m^2 s^{-1}

From the above data, the following diffusion coefficients were obtained by the eigenvalue analysis technique.

D_{11}	D_{12}	D_{21}	D_{22}
(	10^{-9} m^2 s^{-1}		)
2.376	-0.523	-0.262	1.191

REFERENCES

1. R.H. Stokes, J. Am. Chem. Soc., 1950, 72, 763, 2243.
2. R.A. Robinson and R.H. Stokes, Electrolyte Solutions, 2nd Edition, Academic Press, New York, 1959; (a) Chapter 10; (b) Chapter 2; (c) Chapter 7; (d) Chapter 11; (e) Appendix 6.1; (f) Appendix 6.3; (g) p. 31; (h) Appendix 1.1; (i) p. 329.
3. D.G. Leaist and P.A. Lyons, Aust. J. Chem., 1980, 33, 1869.
4. H.S. Harned and D.M. French, Ann. N.Y. Acad. Sci., 1945, 44, 267.
5. D.G. Leaist, J. Chem. Soc., Faraday Trans. I, 1982, 78, 3069.
6. A. Fick, Pogg. Ann., 1855, 94, 59.
7. L. Onsager, Phys. Rev., 1931, 37, 405.
8. L. Onsager, Phys. Rev., 1931, 38, 2265.
9. D.G. Leaist, Can. J. Chem., 1983, 61, 1494.
10. L.W. Barr, D.G. Miller and R. Mills, J. Solution Chem., 1980, 9, 75.
11. A.R. Gordon, J. Chem. Phys., 1937, 5, 522.
12. K.S. Pitzer and G. Mayorga, J. Phys. Chem., 1973, 77, 2300.
13. A.K. Covington, M.I.A. Ferra and R.A. Robinson, J. Chem. Soc., Faraday Trans. I, 1977, 73, 1721.

14. H. Corti, R. Crovetto and R. Fernandez-Prini, J. Solution Chem., 1979, 8, 897.

15. A.D. Fary, Jr. Ph.D. Thesis, Institute of Paper Chemistry (affiliated with Lawrence College), 1966.

16. R.N. Bhatia, K.E. Gubbins and R.D. Walker, Trans. Faraday Soc., 1968, 64, 2091.

17. D.G. Leaist and P.A. Lyons, J. Solution Chem., 1984, 13, 77.

18. L.S. Darken and H.F. Meier, J. Am. Chem. Soc., 1942; 64, 621.

19. W.C. Pierce and E.L. Haenisch, Quantitative Analysis, Wiley, New York, 1948, p. 136.

20. D.A. Skoog and D.M. West, Fundamentals of Analytical Chemistry, 2nd Edition, Holt, Rinehart and Winston, New York, 1969; (a) p. 310; (b) pp. 459-460.

21. H.S. Harned and R.L. Nuttall, J. Am. Chem. Soc., 1947, 69, 736.

22. H.S. Harned, Discuss. Faraday Soc., 1957, 24, 7.

23. T.A. Renner and P.A. Lyons, J. Phys. Chem., 1974, 78, 1667.

24. H.S. Harned and B.B. Owen, The Physical Chemistry of Electrolyte Solutions, 2nd Edition, Reinhold, New York, 1950; (a) p. 250; (b) pp. 381, 385.

25. J.G. Albright and D.G. Miller, J. Phys. Chem., 1975, 79, 2061.

26. J.A. Rard and D.G. Miller, J. Solution Chem., 1979, 8, 755.

27. E.A. Guggenheim and J.C. Turgeon, Trans. Faraday Soc., 1955, 51, 747.

28. H.S. Harned and W.J. Hamer, J. Am. Chem. Soc., 1933, 55, 2194, 4496.

29. H.S. Harned and G.E. Mannweiler, J. Am. Chem. Soc., 1935, 57, 1873.

30. H.S. Harned and H.R. Copson, J. Am. Chem. Soc., 1933, 55, 2206.

31. H.S. Harned and J.G. Donelson, J. Am. Chem. Soc., 1937, 59, 1280.

32. K.S. Pitzer, J. Phys. Chem., 1973, 77, 268.

33. G. Akerlof and P. Bender, J. Am. Chem. Soc., 1948, 70, 2366.

34. R.H. Stokes, J. Am. Chem. Soc., 1945, 67, 1689.

35. G. Akerlof and G. Kegeles, J. Am. Chem. Soc., 1940, 62, 620.

36. H.S. Harned and F.E. Swindells, J. Am. Chem. Soc., 1926, 48, 126.

37. M. Knobel, J. Am. Chem. Soc., 1923, 45, 70.

38. G. Scatchard, J. Am. Chem. Soc., 1925, 47, 648.

39. A. Ferse, Z. Phys. Chem. (Leipzig), 1965, 229, 51.

40. H.S. Harned, J. Am. Chem. Soc., 1925, 47, 676.

41. H.S. Harned and J.C. Hecker, J. Am. Chem. Soc., 1933, 55, 4838.

42. H.S. Harned and M.A. Cook, J. Am. Chem. Soc., 1937, 59, 496.

43. D.G. Leaist and P.A. Lyons, J. Solution Chem., 1981, 10, 95.

44. A. Revzin, J. Phys. Chem., 1972, 76, 3419.

45. E.L. Cussler, Multicomponent Diffusion, Elsevier, Amsterdam, 1976, Chapter 4.

46. P.J. Dunlop, B.J. Steel and J.E. Lane, Experimental methods studying diffusion in liquids, gases, and solids. In Physical Methods of Chemistry, Vol. 1. Edited by A. Weissberger and B.W. Rossiter, Wiley, New York, 1972, p. 205.

47. H. Fujita and L.J. Gosting, J. Phys. Chem., 1960, 64, 1256.

48. J.G. Albright and B.C. Sherril, J. Solution Chem., 1979, 8, 201.

49. D.G. Miller, J. Solution Chem., 1981, 10, 831.

50. E.L. Cussler and P.J. Dunlop, J. Phys. Chem., 1966, 70, 1880.

51. G. Kosanovich and H.T. Cullinan, Can. J. Chem. Eng., 1971, 49, 753.

52. R.P. Wendt, J. Phys. Chem., 1965, 69, 1227.

53. P.J. Dunlop, J. Phys. Chem., 1959, 63, 612.

54. H. Kim, G. Reinfields and L.J. Gosting, J. Phys. Chem., 1973, 77, 934.

55. D.G. Leaist and P.A. Lyons, J. Phys. Chem., 1982, 86, 564.

56. F.T. Wall, P.F. Grieger and C.W. Childers, J. Am. Chem. Soc., 1952, 74, 3562.

57. M. Tanigaki, K. Kondo, M. Harada and W. Eguchl, J. Phys. Chem., 1983, 87, 586.

58. H. Kim, J. Phys. Chem., 1969, 73, 1716.

59. H.L. Toor, AIChE J., 1964, 10, 448, 460.

60. W.E. Stewart and R. Prober, Ind. Eng. Chem. Fundam., 1964, 3, 224.

61. H. Margenau and G.M. Murphy, The Mathematics of Physics and Chemistry, 2nd Edition, Van Nostrand, New York, 1956, p. 320.

62. E.L. Cussler, Ph.D. Thesis, University of Wisconsin, 1965.

63. E.L. Cussler and E.N. Lightfoot, J. Phys. Chem., 1965, 69, 736.

64. L. Onsager and R.M. Fuoss, J. Phys. Chem., 1932, 36, 2689.

65. M. Chen and L. Onsager, J. Phys. Chem., 1977, 81, 2017.

66. L. Onsager, Ann. N. Y. Acad. Sci., 1945, 46, 241.

67. S.R. De Groot and P. Mazur, Non-equilibrium Thermodynamics, North Holland, Amsterdam, 1962.

68. R.A. Noulty and D.G. Leaist, J. Solution Chem., 1984, 13, 767.

69. D.G. Leaist and P.A. Lyons, J. Phys. Chem., 1981, 85, 1756.

70. D. Pletcher, Industrial Electrochemistry, Chapman and Hall, New York, 1982, pp. 128, 186.

71. A.F.W. Cole and A.R. Gordon, J. Phys. Chem., 1936, 40, 733.

72. Y. Awakura, A. Ebata, M. Morita and Y. Kondo, Denki Kaguku, 1975, 43, 569.

73. G.D. Rai and H.T. Cullinan, Jr., J. Chem. Eng. Data, 1973, 18, 213.

74. A. Vogel, Vogel's Textbok of Quantitative Inorganic Analysis, 4th Edition, Revised by J. Basset, R.C. Denney, G.H. Jeffery and J. Mendham, Longman, New York, 1978; (a) pp. 379-380; (b) p. 308.

75. D.G. Leaist, Can. J. Chem., 1985, 63, 2933.

76. D.G. Miller, J.A. Rard, L.B. Eppstein and R.A. Robinson, J. Solution Chem., 1980, 9, 467.

77. W.G. Eversole, H.M. Kindsvater and J.D. Paterson, J. Phys. Chem., 1942, 46, 370.

78. R.A. Noulty and D.G. Leaist, J. Solution Chem., 1987, in press.

79. D.G. Leaist, Can. J. Chem., 1984, 62, 1692.

80. M. Kerker, J. Am. Chem. Soc., 1957, 79, 3664.

81. A.K. Covington, J.V. Dobson and W.F.K. Wynne-Jones, Trans. Faraday Soc., 1965, 61, 2057.

82. K.S. Pitzer, R.N. Roy and L.F. Silvester, J. Am. Chem. Soc., 1977, 99, 4930.

83. G.D. DeLancey, J. Phys. Chem., 1969, 73, 1591.

84. D.G. Leaist, J. Chem. Soc., Faraday Trans. 1, 1987, 83, 829.

85. K.S. Pitzer and L.F. Silvester, J. Solution Chem., 1976, 5, 269.

86. K.S. Pitzer and J.J. Kim, J. Am. Chem. Soc., 1974, 96, 5701.

87. M. Selvaratnam and M. Spiro, Trans. Faraday Soc., 1965, 61, 360.

88. H.S. Harned and R.L. Nuttall, J. Am. Chem. Soc., 1949, 71, 1460.

89. O.W. Edwards and E.O. Huffman, J. Phys. Chem, 1959, 63, 1830.

90. D.G. Leaist, J. Chem. Soc., Faraday Trans. 1, 1984, 80, 3041.

91. R.A. Noulty and D.G. Leaist, J. Phys. Chem., 1987, 91, 1655.

92. D.G. Leaist and R.A. Noulty, Can. J. Chem., 1985, 63, 476.

93. J.A. Harpst, E. Holt and P.A. Lyons, J. Phys. Chem., 1965, 69, 2333.

94. H. Kim, J. Phys. Chem., 1970, 74, 4577.

95. P.L. Vitagliano, C.D. Volpe and V. Vitagliano, J. Solution Chem., 1984, 13, 549.